Point-by-point responses on reviews on "Denitrification in soil as a function of oxygen supply and demand at the microscale" *by* Lena Rohe et al.

We thank the editor and three reviewers very much for the positive opinion and constructive comments on the manuscript.
The authors' answer is in italic font.

Reconsidering our data in detail revealed a mistake in calculating the fluxes of CO_2, N_2O and (N_2O+N_2). This error occurred because of wrong parentheses in the calculation. Correcting the calculation revealed increased values of fluxes by a constant factor compared to the previous values. All calculated fluxes have been corrected, having effects on CO_2, N_2O and (N_2O+N_2) fluxes, N loss and Figure 3, Figure 5 (was removed to Supplementary Material, Figure S6), Figure S1, S3, Table S1 and S4, and the explained variability of N_2O and (N_2O+N_2) fluxes (calculated by the partial least square regression; PLSR) (Figure 7 in revised version), Figure S8 in revised version and Table S2). We want to point out, that the values of fluxes are higher in the revised version, although the course of CO_2, N_2O and (N_2O+N_2) fluxes over incubation time did not change. We apologize very much for this mistake, but the changes made because of the increased fluxes did not affect the interpretation of data or statements of our study.

In the meantime we were able to calculate the ansvf ($ansvf_{cal}$) from parallel incubations using (N_2O+N_2) fluxes during oxic conditions and after switching to anoxic conditions (Supplementary Material, Table S3). Therefore, instead of reporting $ansvf_{cal}$ based on the comparison between oxic and anoxic (N_2O+N_2) fluxes of two different incubation experiments, we now report values based on fluxes of the same experiment which we consider more reliable. Although $ansvf_{cal}$ values changed slightly our previous conclusions remain unchanged.

Anonymous Referee #1
Referee: This manuscript investigated the effects of aggregate size and water saturation on N_2O and N_2 fluxes in two soils with contrasting SOM content by repacked soil cores based ^{15}N tracer incubation in combination with X-Ray computed tomography. The main outcome was that N-gases emissions could be well predicted by considering proxies for oxygen supply (anaerobic soil volume fraction, i.e., ansvf) and demand (CO_2 emissions), which linked the change of soil structure with N-gases emissions. Generally, this manuscript is well prepared and written, and the conclusions were supported by the results of the experiments.

One of my major concerns was that how could one time point (at the end of the incubation) microstructure analysis for the repacked soil cores represent the change of ansvf during the 192 h lasting incubation.

In theory the anaerobic soil volume fraction (ansvf) should be governed by O_2 supply imprinted by the distribution of air-filled pores and modulated locally by the O_2 demand through microbial respiration. The former was estimated from CT derived images after 192 h of incubation using the distance to air filled pores as an estimate caused only by physical conditions, i. e. pore structure (connected air), as explained in the method section (line 224 ff.).
The reviewer is correct in criticizing that we cannot rule out redistribution of water and air during 192 h of incubation. We assume that such redistribution events are typically associated with abrupt changes in local O_2 concentrations as well as CO_2 and N_2O release. The time series data (Figures S1 and S2) show that this may occur occasionally. However, taking

several CT scans during incubation was just not an option due to methodological challenges. Likewise, variations of ansvf due to O_2 demand by local microorganisms (i.e. activity) and over incubation time cannot be estimated. However, in the discussion section variations of ansvf due to O_2 demand were mentioned (line 496 ff. and line 596 ff.).

We assume that there are substantial variation during the first 24 h of incubation, which are omitted from the analysis, but only minor variations after all the genes for denitrification have been expressed and the soil has reached a dynamic equilibrium of O_2 supply and demand and a rather static distribution of water and air. Although microbial activity could affect the ansvf, ansvf largely contributed to explanation of N_2O and (N_2O+N_2) fluxes, in combination with CO_2 release.

Another method was also used to estimate the ansvf ($ansvf_{cal}$, see Supplementary Material) by microbial denitrification activity only. We found accordance between both estimates for RM soil and discussed possible reasons for differences between ansvf and $ansvf_{cal}$ for GI soil.

In the revised version we discussed in more detail that ansvf may be altered by O_2 demand (CO_2 release) and/or O_2 supply during the incubation time of 192 h (l. 496 ff): "The distance threshold for anoxic conditions to emerge was set on an ad-hoc basis at 5 mm from connected air at the end of incubation, but is likely to vary with O_2 demand by local microbial activity (CO_2 release represented by the green fringe area, item 2) during the incubation (Kremen et al., 2005; Rabot et al., 2015; Ebrahimi and Or, 2018; Keiluweit et al., 2018; Kravchenko et al., 2018; Schlüter et al., 2019). Because we could only conduct X-ray CT-scans at the end of incubation, redistribution of water during the incubation time cannot be ruled out. This could have changed ansvf and thus might explain some of the temporal variability of gaseous fluxes."

Referee: In addition, why the aggregate size exhibit no obvious effects on CO2 and denitrification product stoichiometry should be discussed.

In the present study aggregate size did not affect CO_2 release or denitrification and we argued that aggregate radii (1-2 or 2-4 mm) were smaller than the thresholds of distances to connected air that were found to determine the ansvf. The critical distance to estimate the ansvf were selected from best correlations between ansvf and N_2O as well as (N_2O+N_2) fluxes. Results indicated that aggregate size might have been too small to provoke differences in CO_2, N_2O and (N_2O+N_2) fluxes. This point will be considered in more detail in the revised version.

So far we discussed this point in line 503 ff.: "The fact that aggregate size had no effect on denitrification indicates that critical distances were larger than the aggregate radii and rather controlled by air distribution in the macropore system. This is in contrast to the very short critical distances of 180µm for sufficient soil aeration estimated by Kravchenko et al. (2018) and Kravchenko et al. (2019) for intact soil cores containing crop residues for which soil respiration was not determined but likely to be much higher."

Referee: Specific comments Introduction

The challenge for direct measuring soil borne N_2 from soil cores should be mentioned. This info may also provide rational for the authors to use ^{15}N tracer to estimate N_2 flux.

We agree that this point could be better introduced and was rephrased in the updated manuscript as (line 85 ff.):

"Since the N_2 background of air (78%) is very high, direct N_2 measurement from denitrification in soil is very challenging (Groffman et al., 2006; Mathieu et al., 2006). The ^{15}N labelling technique is a method successfully applied to determine N_2O and also N_2 production from denitrification from ^{15}N amended electron acceptors (NO_3^-) (Mathieu et al., 2006; Scheer et al., 2020)." Moreover, we explained that N_2 depleted atmosphere was used to improve N_2 flux detection (l. 82 ff.).

Referee: Results

I suggest move the resulting regression equations from SI to text so that the reader could easily capture the key point of explanatory variables for denitrification.

This is a good remark and we moved the regression equations to the main text in the revised version (Result section, 3.4 Explanatory variables for denitrification, l. 442 ff.).

Referee: Line 23,567 oxygen should be O2

We replaced oxygen with O_2 in the revised version.

Referee: Line 24, I suggest change the order of "ansvf" and "CO2" since "CO2" is more important in terms of explanatory based on the author's results.

We changed the order of CO_2 and ansvf in the revised version.

Referee: Line 119, comma in the sentence should be deleted.

We deleted the comma in the revised version.

Referee: Line 151, why additional nitrate solution was sprayed in the last two treatments? if the N substrates differed among the three treatments, how could the author compared the N2O and N2 flux among the tree treatments?

We agree that this should be clarified and explained in more detail. All treatments contained the same amount of nitrate per mass of soil (50mg/kg soil). Hence the total amount of nitrate per column differed between the two soil types due to different bulk densities. However, the total amount of nitrate did not differ between three saturation levels. 50mg/kg N-KNO_3 was added to the respective amount of water. Hence, for higher water saturations the nitrate concentration in the solution was lower, so that the total amount was the same. This solution was used for moistening the soil. We rephrased as (l. 132 ff.):

"Three different saturation treatments were prepared for subsequent incubation experiments (70%, 83% and 95% WHC) to control the O2 supply and thus provoke differences in denitrification activity. A ^{15}N solution was prepared by mixing 99 at% ^{15}N-KNO_3 (Cambridge Isotope Laboratories, Inc., Andover, MA, USA) and unlabelled KNO_3 (Merck, Darmstadt, Germany) to reach 50 mg N kg^{-1} soil with 60 at% ^{15}N-KNO_3 in each water saturation treatment. Hence, for higher water saturations the stock solution was more diluted in order to reach the same target concentration in the soil. In a first step the soil was adjusted to 70% WHC before packing. […] For the latter two saturation levels the rest of NO_3^- solution was sprayed sequentially onto each layer after packing."

Referee: Line 222, clearly

We replaced "clearaly" by "clearly" in the revised version.

"Only macropores twice this nominal resolution were clearly detectable in the soil core images."

Referee: clearly Line 444-445 the order of the sub figures for the two tested soils was reversed

We corrected this mistake:

"Figure 7: Average O_2 saturation (at the end of incubation experiment) measured with 4 sensors each located at the center of soil core as a function of distance to visible connected air for soil from Gießen (GI, (a)-(c), blue) and Rotthalmünster (RM, (d)-(f), red), and for two aggregate sizes (2-4mm and 4-8mm). (a) and (d) show results for lowest (b) and (e) for medium and (c) and (f) for highest water saturation. The inset in (a), (b), and (d) shows a reduced distance range. The distance to visible connected air is averaged in a spherical region around the sensor tip (7.2 mm diameter). The Spearman's rank correlation coefficient (R) result from Spearman's rank correlation and indicate the extent of monotonic relation between the ranks of both variables. The associated p-values (p) were corrected for multiple comparison according to Benjamini and Hochberg (1995)."

Referee: Line 545 is?

We wrote "as" instead of "is".

"However, there is always a trade-off between retrieving more information and disturbing the soil as little as possible."

Anonymous Referee #2

Denitrification process is of critical importance because it is closely related with agricultural sustainability, environmental quality, and human health. However, the denitrification process in particular N_2O/N_2 generation and emission is poorly understood at microscopic scales. This study provides very useful information towards understanding the complete denitrification process with X-

ray CT imaging analysis, and gives new insights how the N_2O and N_2O+N_2 are formed in soils at microscopic scales.

Major issues/concerns

The authors selected two different land use types of soils when investigating soil organic matter contents. The grassland soil has a SOM up to 4.5%, much higher than that of arable soil. I feel that it is difficult to compare the denitrification process between soils with different land use types. The authors had better use arable soils with different gradients of SOM to investigate the effects of SOM on the complete denitrification process.

> *We acknowledge that grassland and agricultural soil have vastly different soil structure and different input of plant residues. However, these effects are removed after sieving and removal of particulate organic matter and long-term storage. In other words, we did not work with differently managed soil, but rather with soil material with similar texture, but different SOM content, artificially repacked to some target bulk density, so that potential management effects are ruled out.*
>
> *In our experiment we controlled the nitrate content, temperature and water saturation, but could include other measures for oxygen supply and demand, such as soil structure measures that are influenced by the soil texture (i. e. proportion of sand, silt and clay in soil), or CO_2 fluxes that indicate microbial activity. Possibilities to explore complete denitrification with soil organic matter (SOM) were described in detail in the discussion section (l. 576 ff.).*
>
> *However, experiments including variations in temperature, nitrate availability or other properties, like SOM gradients would be very interesting and expand the knowledge on denitrification.*

It is unclear why the authors set up these three different water saturation (70, 83 and95%). The 60% water saturation is widely used when setting up the soil microcosm experiments. I feel that 60% water saturation is needed as the control when setting up the gradients of water saturation experiment in this study.

> *It is true, a lower water saturation is widely used, especially in studies focussing on nitrification or on co-occuring processes like nitrification, nitrifier denitrification and denitrification. It is known from previous studies, that N_2O is produced during nitrification in soil at approximately 70% WFPS (Davidson 1991, Cardenas et al. 2017). This paper focuses on denitrification only. So with a series from 63% to 95% WFPS we capture the transition from low N_2O production through denitrification due to sufficient oxygen supply all the way to low N_2O emission due to further reduction to N_2. Another treatment would not have brought about any additional insights into the microscale mechanisms at play. Moreover, we conducted pre-test with varying WFPS, finding that with these soils, minimum saturation of 75% WFPS was necessary to ensure robust N_2 flux detection.*

Moreover, the flooded paddy soils are widely distributed all over the world, in particular Asian areas. The authors had better include such kind of soil in their experiments to gain a full picture of water saturation effects on the complete denitrification process. The flooded paddy soil usually has a low N_2O emission but a high N_2 emission. It may be an excellent material when investigating the effects of water saturation on the complete denitrification.

> *It is true, that water saturation effects on complete denitrification of paddy soils, in particular differences in N_2O and N_2 emissions following different saturations, is very interesting to analyse, especially when regarding effects of climate change on such anthropogenic systems. However, naturally these flooded or ponded tropical or subtropical soils are exposed to completely different climatic conditions than the selected soils of the presented study. Thus it might be very interesting to include such soils in comparable experiments with temperature gradients as an additional factor for denitrification activity. The current study focussed on*

disentangling structural effects of mineral soils on O_2 supply and O_2 demand, without considering of temperature effects.

We have touched this comment in the section 4.3. (Future directions and implications for modelling) and included in the updated version at the end of this section (l. 606 ff.):

"It would thus be very interesting to include also different soil types and land-use types from various climate zones in future studies, e.g. paddy soils having high water saturation and are known to show a high denitrification activity with N_2 emissions exceeding that of N_2O emissions.

The authors have shown very detailed information in Results section. However, it is difficult for reader to follow in this section. So the authors need to improve this section and lead the readers to pay attention to their important findings.

Thank you for the suggestion. We tried to sharpen the results section by removing the regression analysis of ansvf with different gases into the supporting information and only keeping the essential findings of this regression analysis in the main text. By this, we have removed one figure (Figure 5) and one paragraph from the main paper.

The authors showed their results based on different gradients of distance, water saturation and so on. I feel that they need to show their results with incubation time, at least in supplementary files. They should clarify why they show the results of a specific incubation time in the main body of this manuscript.

Structural measures were only analysed at the end of incubation. CO_2 and N_2O fluxes, O_2 consumption, and product ratios are presented as a function of time in the Supplementary Material (Figure S1, S2 and S5). Average values of CO_2, N_2O and (N_2O+N_2) release of the incubation period (24-192 h) were used for correlations. Average O_2 saturation of the final 24 h was taken for all subsequent analysis, as this probably best reflects the water distribution scanned with X-ray CT (see l. 315 ff.).

Regarding the CT derived measures (e. g. connected air, diffusivity, distance to connected air, ansvf), the reviewer is correct in criticizing that we cannot rule out redistribution of water and air during 192 h of incubation. We assume that such redistribution events are typically associated with abrupt changes in local O_2 concentrations as well as CO_2 and N_2O release. The time series data (Figures S1 and S2) show that this may occur occasionally. However, taking several CT scans during incubation was just not an option due to methodological challenges. Likewise, variations of ansvf due to O_2 demand by local microorganisms (i.e. activity) and over incubation time cannot be estimated. We assume that there are substantial variation during the first 24 h of incubation, which are omitted from the analysis, but only minor variations after all the genes for denitrification have been expressed and the soil has reached a dynamic equilibrium of O_2 supply and demand and a rather static distribution of water and air. Although microbial activity could affect the ansvf, ansvf largely contributed to explanation of average N_2O and (N_2O+N_2) fluxes, in combination with CO_2 release.

Minor issues/concerns

P4 L119: delete the comma after N2O.

We deleted the comma in the revised version.

P5 L150-151: is added nitrate amounts equal for each treatment?

We agree that this should be clarified and explained in more detail. All treatments contained the same amount of nitrate per mass of soil (50mg/kg soil). Hence the total amount of nitrate per column differed between the two soil types due to different bulk densities. However, the total amount of nitrate did not differ between three saturation levels. 50mg/kg N-KNO_3 was added to the respective amount of water. Hence, for higher water saturations the nitrate concentration in the solution was lower, so that the total amount was the same. This solution was used for moistening the soil. We rephrased as (l. 132 ff.):

"Three different saturation treatments were prepared for subsequent incubation experiments (70%, 83% and 95% WHC) to control the O_2 supply and thus provoke differences in denitrification activity. A ^{15}N solution was prepared by mixing 99 at% ^{15}N-KNO_3 (Cambridge Isotope Laboratories, Inc., Andover, MA, USA) and unlabelled KNO_3 (Merck, Darmstadt, Germany) to reach 50 mg N kg^{-1} soil with 60 at% ^{15}N-KNO_3 in each water saturation treatment. Hence, for the two higher water saturations the stock solution was more diluted in order to reach the same target concentration in the soil. In a first step the soil was adjusted to 70% WHC before packing. […]For the latter two saturation levels the rest of NO_3^- solution was sprayed sequentially onto each layer after packing."

P24 L630-633: please clarify this sentence.

This sentence was removed without loss.

Anonymous Referee #3

This study aimed to explore the controlling factors (soil organic matter, aggregate size, water saturation) of the denitrification process (N2O/N2) at microscopic scale using new approaches of X-ray computed tomography and 15N tracer incubation. They found that N2O/N2 fluxes could be well predicted by anaerobic soil volume fraction (ansvf, O2 supply) and CO2 release (O2 demand). This findings would expand our understanding of how the N2O and N2 are formed in soils. In general, the experimental design is clear, and the manuscript is well written. However, there are some concerns about the methodology and data interpretation.

Major comments

1.The authors selected two types of soils with contrasting soil properties, including soil organic matter contents, soil texture, soil pH and etc., so it is unclear why the authors concluded the differences in denitrification (N2O and N2O+N2 fluxes) between two investigated soils were triggered by different respiration rates due to different SOM content rather than other properties.

Main drivers for soil respiration are temperature, water saturation, oxygen saturation and nutrient content / availability. Soil types in turn affect soil structure, i. e. water saturation and oxygen saturation, and nutrient availability. The temperature was set at 20 °C during the incubation experiment and the water saturation was controlled in parallel experiments (70, 83, 90 % WHC). It is true, that soil texture or soil pH might affect the nutrient storage and thus availability for microbes, but nitrate as the electron acceptor for denitrification was supplied sufficiently in the presented experiment. Thus we could exclude the availability of nitrate, temperature effects, or water saturation in our analysis. In the revised version we included, that a recent study by Malique et al. (2019) investigated the denitrification potential of both soils (RM and GI) and found a higher denitrification potential with GI soil compared to that of RM soil. This finding emphasizes that soil texture and bulk density should mainly govern air content and thus O_2 supply at a certain water saturation, whereas SOM content should mainly govern microbial activity and thus O_2 demand and energy sources for denitrifiers. We fully account for bulk density differences through its effect on air content and air distribution at a given water saturation. This is assessed by proxies for O_2 supply.

We described controlled or excluded factors at the beginning of the discussion as follows (l. 471 ff.): "This study was designed to examine different levels of O_2 consumptions by comparing soils with different SOM contents and different levels of O_2 supply by comparing different aggregate sizes and different water saturations. Other factors that would have affected O_2 demand and energy sources for denitrifiers (quality of organic matter, temperature, pH, plant-soil interactions), O_2 supply (oxygen concentration in the headspace,

temperature) or other drivers of denitrification (NO_3^- concentration, pH, denitrifier community structure) were either controlled or excluded in this study. "

However, experiments including variations in temperature, nitrate availability and/or other properties, like SOM or soil structure, would be very interesting and expand the knowledge on denitrification.

2. In the results section, the authors displayed the averages for the whole incubation, I feel it is better to show their results with incubation time. And of course, I also think it is not so reasonable to correlated average gas fluxes to the X-ray CT data of a specific incubation time, because the fluxes are not constant during incubation, neither for anaerobic soil volume fraction.

Structural measures were only analysed at the end of incubation. CO_2 and N_2O fluxes, O_2 consumption, and product ratios are presented as a function of time in the Supplementary Material (Figure S1, S2 and S5). Average values of CO_2, N_2O and (N_2O+N_2) release of the incubation period (24-192h) were used for correlations. Average O_2 saturation of the final 24h was taken for all subsequent analysis, as this probably best reflects the water distribution scanned with X-ray CT (see line 315 ff.).

Regarding the CT derived measures (e. g. connected air, diffusivity, distance to connected air, ansvf), the reviewer is correct in criticizing that we cannot rule out redistribution of water and air during 192 h of incubation. We assume that such redistribution events are typically associated with abrupt changes in local O_2 concentrations as well as CO_2 and N_2O release. The time series data (Figures S1 and S2) show that this may occur occasionally. However, taking several CT scans during incubation was just not an option due to methodological challenges. Likewise, variations of ansvf due to O_2 demand by local microorganisms (i.e. activity) and over incubation time cannot be estimated (line 496 ff.).

We assume that there are substantial variation during the first 24 h of incubation, which are omitted from the analysis, but only minor variations after all the genes for denitrification have been expressed and the soil has reached a dynamic equilibrium of O_2 supply and demand and a rather static distribution of water and air. Although microbial activity could affect the ansvf, ansvf largely contributed to explanation of N_2O and (N_2O+N_2) fluxes, in combination with CO_2 release.

3. From the detailed information showed in supplementary file, the variation between three replicates is very large (eg. Figure S1), the reasons for this large variation as well as the effects on the data reliability need to be clarify.

We can only assume possible reasons for the observed variations between replicates, but since the replicates were treated very similar according to the described protocol we cannot clearly identify reasons. The only explanation that we found was that small differences in repacking the moistened soil aggregates occurred between replicates (i. e. compaction, distribution of pores, and connectivity of pores), and possibly heterogeneity in the content of organic matter fractions in the aggregates. These small differences may largely affect soil aeration und thus microbial activity.

As can be clearly seen in Figure S4, repacking the aggregates in 2 cm intervals affected the visible air content and also ansvf. Both measures largely differed among replicates incubated at medium saturation for GI and RM soil. This was also pointed out in the result section 3.2, l 350 ff..

For CO_2 emission it was discussed in line 300 ff.: "The variability in CO_2 fluxes between replicates is much higher than the temporal variability during incubation. This is probably explained by small differences in packing of the columns that can have large consequences for soil aeration."

The same explanation was given for N_2O and (N_2O+N_2) emissions in line 305 ff.: "The huge variability between replicates is again higher than the temporal variability (e.g. in Figure 4d

and time series in Supplementary Material, Figure S1) and the effect of aggregate size is inconsistent due to the large variability among replicates." Additionally, small variations in N_2O emissions may result from co-occuring N_2 emissions during denitrification.

Regarding the O_2 saturation averages of the last 24h of incubation were used for correlations and statistical analysis, because we assumed best accordance of the O_2 averages and water distribution (connected air content and ansvf) analysed by CT image analysis at the end of the experiment. The reliability of O_2 saturation data was discussed in the results section (l. 316 ff.): "Average O_2 saturation was lowest with highest water saturation and roughly the same for saturations <80%WFPS (Figure 3b). Some sensors showed a gradual decline in O_2 concentration, whereas some showed a drastic reduction or increase in a short period of time, probably due to water redistribution (Supplementary Material, Figure S2). The average of the final 24h was taken for all subsequent analysis, as this probably best reflects the water distribution scanned with X-ray CT. Standard errors among the seven O_2 microsensors were high in each treatment due to very local measurement of O_2 that probed very different locations in the heterogeneous pore structure."

We think that the data are reliable and comparable, because CO_2, N_2O and (N_2O+N_2) emissions and O_2 saturation as well as the other explanatory variables of the present study were measured for each replicate. Thus, small variations in connected air content or ansvf affect denitrification and respiration in one soil core.

4. And of course it would have been of interest to see the variations in denitrifying communities at microscopic scale.

We agree that this information would be very interesting and helpful for interpretation of results. However, we have presented a very comprehensive experimental setup, combining gas flux measurements, isotopic analysis, image analysis of CT derived data as well as simulating the diffusivity. These were very time consuming methods, especially the demanding image analysis. Methods to analyse the denitrifying communities in soil are not established in our lab and unfortunately we were not able to perform genetic analysis. In the revised version the microbial community was added to the other factors altering denitrification under field conditions in the section 4.3 "Future directions and implications for modelling" (l. 606 ff.).

Minor comments:

L125: The soil depth of topsoil should be define, 0-20 cm?

This information was included as follows (l. 117 ff.): "Fine-textured topsoil material was collected from two different agricultural sites in Germany (from a depth of 10 - 20 cm in Rotthalmünster (RM) and of 3 - 15 cm in Gießen (GI) as representatives for agricultural mid-European soils (Table 1).

L141: How much soil is used for each column?

The target bulk density was 1.3 g cm^{-3} for RM soil and 1.0 g cm^{-3} for GI soil (Table 1). Thus 902 g dry weight of RM soil and 694 g dry weight of GI soil were used per column.

In line 145, we included: "This packing resulted in 902 and 694 g dry weight of RM and GI soil, respectively."

How about the soil depth of the repacked soil cores?

The height of the repacked soil cores was 10 cm. This information is provided in line 141 and Figure 1.

How to control the compactness of filling?

We repacked the soil in five 2 cm intervals (l. 141 ff.).

"This ^{15}N-labelled soil was filled in 2 cm intervals into cylindrical PVC columns (9.4cm inner diameter x10cm height) (Figure 1) and compacted to a target bulk density that correspond to site-specific topsoil bulk densities (Jäger et al., 2003; John et al., 2005)."

L150-151: Why spray additional nitrate solution in 83% and 95% WHC treatments but not in 70% WHC?

We agree that this should be clarified and explained in more detail. All treatments contained the same amount of nitrate per mass of soil (50mg/kg soil). Hence the total amount of nitrate per column differed between the two soil types due to different bulk densities. However, the total amount of nitrate did not differ between three saturation levels. 50mg/kg N-KNO_3 was added to the respective amount of water. Hence, for higher water saturations the nitrate concentration in the solution was lower, so that the total amount was the same. This solution was used for moistening the soil. We rephrased as (l. 132 ff.):

"Three different saturation treatments were prepared for subsequent incubation experiments (70%, 83% and 95% WHC) to control the O_2 supply and thus provoke differences in denitrification activity. A ^{15}N solution was prepared by mixing 99 at% ^{15}N-KNO_3 (Cambridge Isotope Laboratories, Inc., Andover, MA, USA) and unlabelled KNO_3 (Merck, Darmstadt, Germany) to reach 50 mg N kg^{-1} soil with 60 at% ^{15}N-KNO_3 in each water saturation treatment. Hence, for the two higher water saturations the stock solution was more diluted in order to reach the same target concentration in the soil. In a first step the soil was adjusted to 70% WHC before packing. […] Packing in five vertical intervals achieved a uniform porosity across the column. However, there were inevitable porosity gradients within intervals (Figure S4) that affected the air and water distribution and thus air continuity at high water saturations. This packing resulted in 902 and 694 g dry weight of RM and GI soil, respectively. For the latter two saturation levels the rest of NO_3^- solution was sprayed sequentially onto each layer after packing."

The editor has some minor concerns

(1) Pls briefly why upland soil is selected because grassland and arable soils are often exposed to the atmosphere containing approximately 20% oxygen. Therefore, it seems that denitrifiers may be favored only in the microanaerobic site. This kind of upland soil may be dominated by aerobic process, particularly for the surface soil.

The soils were selected as representatives for agricultural mid-European soils. Previous studies with topsoil from Gießen could already prove its denitrification potential (e. g. Müller et al. (2002); Müller et al. (2014)). Studies focussing on organic matter dynamics showed a high microbial activity in topsoil from Rotthalmünster (e. g. John et al. (2005), Helfrich et al. (2006)). Thus we assume a high denitrification potential under O_2 depleted conditions. Denitrification activity was recently investigated and proved by Malique et al. (2019).

Although topsoil communities are exposed to O_2 enriched environments in general, temporal O_2 depletion also occurs following rain events or freeze/thaw cycles. Thus, under O_2 depleted conditions specialized microbial organisms are capable to switch from aerobic respiration to denitrification, which is a facultative anaerobic process. It is well known that in soil with ≥ 60% WFPS different processes co-occur, such as nitrification, nitrifier denitrification and denitrification. This is the reason why we assumed a denitrification potential in the topsoil of both soils that is dependent on the O_2 availability.

We added this point in the Material & Method section as follows (l. 117 ff.): "Fine-textured topsoil material was collected from two different agricultural sites in Germany (from a depth of 10 - 20 cm in Rotthalmünster (RM) and of 3 - 15 cm in Gießen (GI) as representatives for agricultural mid-European soils (Table 1). Malique et al. (2019) recently investigated the denitrification potential of both soils and found a higher denitrification activity with GI soil compared to that of RM soil."

(2) Pls add few sentences for future study about microbial communities. The implicit assumption of this study is that similar community structure of microbiomes exist in physiochemically distinct soils, leading to similar responsive patterns under oxygen and substrate supply. This is also somehow astonishing. At least the flux pattern are largely similar, which may represent similar communities?

The three different water saturations affect the microbial community directly, i. e. switching from aerobic to anaerobic respiration with high water saturation. Although we have no information on the microbial community structure in both soils we were aware that microbial groups had to adapt (i. e. expression of denitrification genes as a response to O_2 depletion) to changes in environmental conditions after raising the water saturation. This was the reason for excluding gas fluxes of the initial 24h of incubation as we accounted this as an equilibrium phase. However, as we have no information on this, we did not assume that the microbial community structure is similar in both soils, but assumed a relatively *short-term expression of the respective genes for denitrification of facultative anaerobic organisms as a response of changing the O_2 conditions. Unfortunately, we could not assess the diversity of microorganisms involved in denitrification in the present study. However, we accounted the higher CO_2, N_2O or (N_2O+N_2) fluxes from GI soil compared to that from RM soil as differences in microbial activity and stated in l. 123 ff. that the "SOM content should mainly govern microbial activity and thus O_2 demand".*

We inserted that microbial structure has to be taken into account in l. 604 ff. "Under field conditions this impact on denitrification is additionally altered by saturation changes, temperature variations, atmospheric gas concentrations, microbial community structure, and plant growth." As we have no information on the microbial community structure we provided this information in line 473 ff. as follows: "Other factors that would have affected O_2 demand and energy sources for denitrifiers (quality of organic matter, temperature, pH, plant-soil interactions), O_2 supply (oxygen concentration in the headspace, temperature) or other drivers of denitrification (NO_3^- concentration, pH, denitrifier community structure) were either controlled or excluded in this study."

(3) Why not use destructive sampling for microstructure analysis. Yes, one time point result cannot represent the entire incubation period, and why destructive sampling could be conducted to have a time-series analysis of microstructure and ansvf? For example, microbial activity could likely reach a high level after incubation for 24 hours, and stayed largely at a plateau level after incubation for 192 hours. In addition, strong respiration may lead to the growth of microorganisms which in turn generate extracellular enzymes or extracellular polymer substance EPS, which could likely significantly distort the soil microstructure and ansvf?

Thank you for this comment. However, due to the experimental setup, it was only possible to scan the soil cores with X-ray CT once directly after the incubation experiment. The soil core was installed in a closed system, including flushing the headspace. Destructive sampling in-between the incubation was thus impossible as it would have affected the whole gas measurements and also the bulk soil mass of one soil core and this would affect the image analysis. Thus, parallel incubations would be the only option to sample microstructure or microbial community during the incubation period. Unfortunately, it was just impossible to run such a complex experimental setup with even more treatments during the project time of 3 years. In total we had 36 incubation vessels (2 soils x 2 aggregate sizes x 3 water saturations) that were incubated over 9 days and carried out in two working weeks. This resulted already in 72 weeks of incubations. Unfortunately, additional vessels to perform destructive sampling of parallel samples would have been too time consuming, although as you also argued it would have provided additional and important information. Please note that X-ray CT is not suitable to detect the release of enzymes and EPS and that it is very unlikely that those

compounds would change the soil structure. If anything they would change structural stability, but there are no mechanical stresses during incubation for which aggregate stability would be relevant.

(4) Can the authors specify the relationship between the volume of a single cell (or population) and the aggregate size. Or in other words, what is the population size of cell that can colonize different aggregates

*We did not perform any microbial or genetic based method. Watt et al. (2006) found 10^7-10^{12} of microbial cells in one gram soil. It is well known that colonization depends on substrate, oxygen and water availability, as summarized by Sessitsch et a. 2001. In the presented study we used macroaggregates (i. e. 2-4 and 4-8 mm), and both aggregate sizes were assumed to provide variations in O_2 supply for microorganisms inhabiting the aggregates. Juyal et al. (2018) performed experiments using sterilized repacked soils of two different aggregate sizes inoculated with two bacterial strains (*Bacillus sp. *and* Pseudomonas sp.*). They found higher cell numbers of* Bacillus sp. *in smaller aggregates (1-2mm) compared to the larger ones (2-4 mm) and attributed this to better nutrient availability in smaller aggregates. However, with the second bacteria* Pseudomonas sp. *they did not find such effects of aggregate sizes and this was in line with previous results by Drazkiewicz (1994). These results indicate that aggregates sizes affect growth of microbial species differently and consequently we cannot provide estimates for cell numbers under presented experimental conditions. Further experiments would be necessary to answer this question.*

Although microbial growth of cell number within different aggregate sizes might be different, we did not find aggregate effects on denitrification and in l. 578 ff. we focussed on this point as follows: "The fact that aggregate size had no effect on denitrification indicates that critical distances were larger than the aggregate radii and rather controlled by air distribution in the macropore system. This means that both aggregate sizes used in the present study might have been too small to provoke differences in CO_2, N_2O and (N_2O+N_2) fluxes. The large distance found here is in contrast to the very short critical distances of 180 µm for sufficient soil aeration estimated by Kravchenko et al. (2018) and Kravchenko et al. (2019) for intact soil cores containing crop residues for which soil respiration was not determined but likely to be much higher."

References:

Drazkiewicz, M.: Distribution of microorganisms in soil aggregates - Effect of aggregate size, Folia Microbiol., 39, 276-282, 10.1007/bf02814312, 1994.

Helfrich, M., Ludwig, B., Buurman, P., and Flessa, H.: Effect of land use on the composition of soil organic matter in density and aggregate fractions as revealed by solid-state ^{13}C NMR spectroscopy, Geoderma, 136, 331-341, https://doi.org/10.1016/j.geoderma.2006.03.048, 2006.

John, B., Yamashita, T., Ludwig, B., and Flessa, H.: Storage of organic carbon in aggregate and density fractions of silty soils under different types of land use, Geoderma, 128, 63-79, https://doi.org/10.1016/j.geoderma.2004.12.013, 2005.

Juyal, A., Eickhorst, T., Falconer, R., Baveye, P. C., Spiers, A., and Otten, W.: Control of pore geometry in Soil microcosms and its effect on the growth and spread of Pseudomonas and Bacillus sp, Frontiers in Environmental Science, 6, 12, 10.3389/fenvs.2018.00073, 2018.

Malique, F., Ke, P., Boettcher, J., Dannenmann, M., and Butterbach-Bahl, K.: Plant and soil effects on denitrification potential in agricultural soils, Plant and Soil, 439, 459-474, 10.1007/s11104-019-04038-5, 2019.

Müller, C., Martin, M., Stevens, R. J., Laughlin, R. J., Kammann, C., Ottow, J. C. G., and Jäger, H. J.: Processes leading to N_2O emissions in grassland soil during freezing and thawing, Soil Biol. Biochem., 34, 1325-1331, 2002.

Müller, C., Laughlin, R. J., Spott, O., and Rütting, T.: Quantification of N_2O emission pathways via a ^{15}N tracing model, Soil Biol. Biochem., 72, 44-54, http://dx.doi.org/10.1016/j.soilbio.2014.01.013, 2014.

Watt, M., Hugenholtz, P., White, R., and Vinall, K.: Numbers and locations of native bacteria on field-grown wheat roots quantified by fluorescence in situ hybridization (FISH), Environmental Microbiology, 8, 871-884, 10.1111/j.1462-2920.2005.00973.x, 2006.

List of relevant changes

- *We used the MS Word template.*
- *One reference was added to the introduction (l. 41):*
  Tian et al. 2020: A comprehensive quantification of global nitrous oxide sources and sinks, Nature, 586, 248-256, 10.1038/s41586-020-2780-0, 2020
- *We explained that N_2 depleted atmosphere was used to improve N_2 flux detection (line 173 ff.): "This artificial atmosphere with low N_2 background concentration was used to increase sensitivity for N_2 fluxes (Lewicka-Szczebak et al., 2017)."*

Denitrification in soil as a function of oxygen supply and demand at the microscale

Lena Rohe[1], Bernd Apelt[1], Hans-Jörg Vogel[1], Reinhard Well[2], Gi-Mick Wu[3], Steffen Schlüter[1]

[1]Helmholtz Centre for Environmental Research – UFZ, Department Soil System Sciences, Theodor-Lieser ~~-5-~~Str. 4, 06120 Halle, Germany

[2]Thünen Institute of Climate Smart Agriculture, Bundesallee 65, 38116 Braunschweig, Germany

[3]Helmholtz Centre for Environmental Research – UFZ, PACE, Permoserstraße 15, 04318 Leipzig, Germany

Correspondence to: Lena Rohe, (lena.rohe@ufz.de)

Abstract

The prediction of nitrous oxide (N_2O) and of dinitrogen (N_2) emissions formed by biotic denitrification in soil is notoriously difficult, due to challenges in capturing co-occurring processes at microscopic scales. N_2O production and reduction depend on the spatial extent of anoxic conditions in soil, which in turn are a function of oxygen (O_2) supply through diffusion and O_2 demand by respiration in the presence of an alternative electron acceptor (e.g. nitrate).

This study aimed to explore controlling factors of complete denitrification in terms of N_2O and (N_2O+N_2) fluxes in repacked soils by taking micro-environmental conditions directly into account. This was achieved by measuring micro-scale oxygen saturation and estimating the anaerobic soil volume fraction (*ansvf*) based on internal air distribution measured with X-ray computed tomography (X-ray CT). O_2 supply and demand was explored systemically in a full factorial design with soil organic matter (SOM, 1.2 and 4.5%), aggregate size (2-4 and 4-8 mm) and water saturation (70, 83 and 95% WHC) as factors. CO_2 and N_2O emissions were monitored with gas chromatography. The ^{15}N gas flux method was used to estimate the N_2O reduction to N_2.

N-gas emissions could only be predicted well, when explanatory variables for O_2 demand ~~supply~~ and ~~oxygen~~ O_2 supply ~~demand~~ were considered jointly. Combining CO_2 emission ~~*ansvf*~~ and *ansvf* ~~CO_2 emission~~ as proxies of O_2 ~~supply~~ demand and ~~demand~~ supply resulted in 83% explained variability in (N_2O+N_2) emissions and together with the denitrification product ratio [$N_2O/(N_2O+N_2)$] (*pr*) ~~72~~81% in N_2O emissions. O_2 concentration measured by microsensors was a poor predictor due to the variability in O_2 over small distances combined with the small measurement volume of the microsensors. The substitution of predictors by independent, readily available proxies for O_2 demand (SOM) ~~O_2 supply (diffusivity)~~ and O_2 supply (diffusivity) ~~O_2 demand (SOM)~~ reduced the predictive power considerably (~~50~~60% and ~~58~~66% for N_2O and (N_2O+N_2) fluxes, respectively).

The new approach of using X-ray CT imaging analysis to directly quantify soil structure in terms of *ansvf* in combination with N_2O and (N_2O+N_2) flux measurements opens up new perspectives to estimate complete denitrification in soil. This will also contribute to improving N_2O flux models and can help to develop mitigation strategies for N_2O fluxes and improve N use efficiency.

Keywords: anaerobic soil volume fraction, air distance, diffusivity, nitrous oxide, dinitrogen, oxygen microsensors, product ratio, X-Ray computed tomography (X-ray CT)

1. Introduction

Predicting emissions of the greenhouse gas nitrous oxide (N_2O) is important in order to develop mitigation strategies. Agriculture accounts for approximately 60% of anthropogenic N_2O emissions, most likely because high amounts of substrates for N_2O producing processes result from nitrogen (N) fertilization on agricultural fields (Syakila and Kroeze, 2011; Thompson et al., 2019; Tian et al., 2020). The required process understanding is hindered, since various microbial species are capable of N_2O production via several pathways and these may co-exist due to different micro-environmental conditions within short distances in soil (Hayatsu et al., 2008; Braker and Conrad, 2011). Denitrification is one of the major biological pathways for N_2O production, which describes the reduction of nitrate (NO_3^-) as the alternative electron acceptor into the trace gas nitrous oxide (N_2O) as an intermediate and molecular nitrogen (N_2) as the final product (Knowles, 1982; Philippot et al., 2007). Although it is well known that not all microbial species are capable of denitrification pathway, it is particularly widespread among bacteria, but also several fungi and even archaea can denitrify (Shoun et al., 1992; Cabello et al., 2004).

N_2O emissions from soils are often considered to be erratic in nature due to their high variability in space and time (Butterbach-Bahl et al., 2013). The low predictability is caused by the mechanisms that regulate microbial denitrification at the pore scale which are concealed from measurement techniques that average across larger soil volumes. This experimental study is designed to reveal the drivers of oxygen (O_2) supply and demand at the microscale that govern microbial denitrification at the macroscale.

In general, there are several controlling factors for microbial denitrification in soil. Proximal factors, such as N and carbon (C) are needed to ensure the presence of electron acceptors and electron supply. In addition, the absence of oxygen is required to express the enzymes for the reduction of reactive nitrogen. Distal factors, i.e. physical and biological factors like soil structure, soil texture, pH or microbial community, on the other hand affect the proximal factors (Groffman and Tiedje, 1988; Tiedje, 1988). The main physical controlling factors that regulate O_2 supply are water saturation and soil structure, because they determine the pathways through which gaseous and dissolved oxygen, but also NO_3^- and dissolved organic matter may diffuse towards the location of their consumption. Likewise they determine the pathways through which denitrification products may diffuse away from these locations. In addition, both, saturation and soil structure, contribute to the regulation of O_2 demand through their impact on substrate accessibility and thus microbial activity (Keiluweit et al., 2016). Studies have shown microbial activity, described by microbial respiration, to increase with increasing water saturation, but it also decreased when water saturation exceeded a certain optimal value at intermediate conditions (Davidson et al., 2000; Reichstein and Beer, 2008; Moyano et al., 2012). Low water saturation causes C substrate limitations whereas high water saturation causes limited oxygen diffusion (Davidson et al., 2000). This observation goes along with an increase of anaerobic respiration in microbial hot spots when O_2 demand exceeded O_2 supply and denitrification is favoured (Balaine et al., 2015).

These physical processes that govern denitrification at the microscale have to be effectively described by macroscopic bulk soil properties in order to improve the predictability of denitrification activity at larger scales. It has been shown repeatedly that soil diffusivity can be used to predict the impact of O_2 supply on N_2O and N_2 emissions (Andersen and Petersen, 2009; Balaine et al., 2016). First N_2O emissions increase with decreasing diffusivity, but then it dramatically decreases due to N_2 production when diffusivity is extremely low.

Diffusivity is not routinely measured in denitrification studies as it is more difficult to measure than air content or water saturation, but there are many empirical models to estimate diffusivity based on air filled pore volume (Millington and Quirk, 1960; Millington and Quirk, 1961; Moldrup et al., 1999; Deepagoda et al., 2011). All of these metrics are only indirect metrics of the anaerobic soil volume fraction (*ansvf*) as direct measurements are difficult to obtain. Either it is measured locally via oxygen sensors with needle-type microsensors (Sexstone et al., 1985; Højberg et al., 1994; Elberling et al., 2011) or with foils (Elberling

Kommentar [LR1]: Added reference: Tian et al. 2020

et al., 2011; Keiluweit et al., 2018), which requires to average or to extrapolate measured O_2 saturation for the entire soil volume. Or it is estimated for the entire sample volume from pore distances in X-ray CT images of soil structure assuming that there is a direct relationship between pore distances and anaerobiosis (Rabot et al., 2015; Kravchenko et al., 2018).

Completeness of denitrification is another important controlling factor that modulates the relationship between ~~oxygen~~ O_2 availability and N_2O emissions (Morley et al., 2014) which has previously been neglected in similar incubation studies (Rabot et al., 2015; Porre et al., 2016; Kravchenko et al., 2018). ~~due to methodological challenges imposed by measuring N_2 emissions from soil (Groffman et al., 2006).~~ Since the N_2 background of air (78%) is very high, direct N_2 measurement from denitrification in soil is very challenging (Groffman et al., 2006; Mathieu et al., 2006). The ^{15}N labelling technique is a method successfully applied to determine N_2O and also N_2 production from denitrification from ^{15}N amended electron acceptors (NO_3^-) (Mathieu et al., 2006; Scheer et al., 2020). Complete denitrification generates N_2 as the final product although it is assumed that 30% of denitrifying organisms lack the N_2O reductase (Zumft, 1997; Jones et al., 2008; Braker and Conrad, 2011). Thus the denitrification product ratio $[N_2O/(N_2O+N_2)]$ (*pr*) was found to be very variable in soil studies covering the whole range between 0 and 1 (Senbayram et al., 2012; Buchen et al., 2016). Decreasing *pr*, i.e. relative increasing N_2 fraction compared to that of N_2O, were found with lower oxygen availability in consequence of higher water saturations and denitrification activities in soil (van Cleemput, 1998).

In this paper, we will reconcile all these metrics, i.e. soil structure, bulk respiration, diffusivity, O_2 distribution, *ansvf* and *pr* to assess their suitability to predict denitrification activity. This requires well defined laboratory experiments that either control or directly measure important distal controlling factors of denitrification activity like microbial activity, anaerobic soil volume and denitrification completeness.

To this end the current study presents a comprehensive experimental setup with well-defined experimental conditions but also micro-scale measurements of oxygen concentrations, soil structure and the air and water distribution at the pore scale. The ^{15}N tracer application was used to estimate the N_2O reduction to N_2 and the N_2O fraction originating from denitrification. To our knowledge this is the first experimental setup analyzing N_2O and (N_2O+N_2) fluxes in combination with X-ray CT derived structure. Other important factors controlling denitrification like temperature, pH, nitrate limitation, saturation changes, microbial community structure, or plant-soil interactions were either controlled or excluded in this study.

The general objective of the present study is to systematically explore bulk respiration and denitrification as a function of O_2 supply and demand in repacked soils under static hydraulic conditions. O_2 demand was controlled by incubating soils with different soil organic matter (SOM) content. O_2 supply was controlled by different water saturations and different aggregate sizes. A novel approach is explored to assess microscopic O_2 supply directly from *ansvf* estimates based on the distribution and continuity of air-filled pores within the wet soil matrix.

We hypothesize that the combination of at least one proxy for O_2 supply (e.g. *ansvf*, diffusivity, air content) and one for O_2 demand (CO_2 production) is required to predict complete denitrification (N_2O+N_2), whereas *pr* as a proxy for denitrification completeness is required in addition to predict a single component (N_2O). ~~,~~ The specific aims of our study were a) to investigate the potential of microscopic metrics for O_2 supply such as *ansvf* to predict complete denitrification activity and b) to explore as to how far a substitution of these predictors by classical, averaged soil properties required for larger scale denitrification models is acceptable.

2. Materials and Methods

2.1 Incubation

Fine-textured topsoil material was collected from two different agricultural sites in Germany (from a depth of 10 - 20 cm in Rotthalmünster (RM) and 3 - 15 cm in Gießen (GI) as representatives for agricultural mid-European soils~~,~~ (Table 1). Malique et al. (2019) recently investigated the denitrification potential of both soils and found a higher denitrification activity with GI soil compared to that of RM soil. According to this, ~~These~~ these soils were chosen for the contrast in properties potentially affecting denitrification and respiration (SOM contents, pH, texture, bulk density) which induces a large difference in microbial respiration and hence O_2 demand under identical incubation settings. The rationale was that soil texture and bulk density should mainly govern air content and thus O_2 supply at a certain water saturation, whereas SOM content should mainly govern microbial activity and thus O_2 demand. The soils were sieved (10 mm), air-dried and stored at 6°C for several months before sieving into two different aggregate size fractions in order to induce variations in O_2 supply: small (2-4 mm) and large (4-8 mm). Care was taken to remove free particulate organic matter (POM) like plant residues and root fragments during sieving. Other aggregate size classes were not considered, as sieving yielded in a too low amount of larger aggregates that contained too much irremovable POM, whereas smaller aggregate classes resulted in a too fragmented pore space at the chosen scan settings.

Table 1: Basic description of soil materials used for incubation (SOM – soil organic matter).

Site	Land use	Soil type (WRB)	Bulk density [g/cm³]	Clay [%]	Silt [%]	SOM [%]	C:N	pH ($CaCl_2$)
Rotthalmünster (RM)	arable	Luvisol	1.3	19	71	1.21	8.7	6.7
Gießen (GI)	grassland	Gleysol	1.0	32	41	4.46	10.0	5.7

The soil material was pre-incubated at 50% water holding capacity (WHC) for two weeks to induce microbial activity after the long dry spell and let the flush in carbon mineralization pass that occurs after rewetting the soil. Three different saturation treatments were prepared for subsequent incubation experiments~~:~~ (70%, 83% and 95% WHC) to control the O_2 supply and thus provoke differences in denitrification activity. A ^{15}N solution was prepared by mixing 99 at% ^{15}N-KNO_3 (Cambridge Isotope Laboratories, Inc., Andover, MA, USA) and unlabelled KNO_3 (Merck, Darmstadt, Germany) to reach 50 mg N kg^{-1} soil with 60 at% ^{15}N-KNO_3 in each water saturation treatment. ~~Three different saturation treatments were prepared for subsequent incubation experiments: 70%, 83% and 95% WHC.~~ Hence, for the two higher water saturations the stock solution was more diluted in order to reach the same target concentration in the soil. In a first step the soil was adjusted to 70% WHC before packing.

~~^{15}N labeled NO_3^- solution was applied when adjusting WHC to 70% before packing by mixing 99 at% ^{15}N-KNO_3 (Cambridge Isotope Laboratories, Inc., Andover, MA, USA) and unlabelled KNO_3 (Merck, Darmstadt, Germany) to reach 50 mg N kg^{-1} soil and 60 atom%.~~ This ^{15}N-labelled soil was filled in 2 cm intervals into cylindrical PVC columns~~-~~ (9.4cm inner diameter x 10cm height) (Figure 1) and compacted to a target bulk density that correspond to site-specific topsoil bulk densities (Jäger et al., 2003; John et al., 2005). Packing in five vertical intervals achieved a uniform porosity across the column. However, there were inevitable porosity gradients within intervals (Figure S4) that affected the air and water distribution and thus air continuity at high water saturations. This packing resulted in 902 and 694 g dry weight of RM and GI soil, respectively. For the latter two saturation levels the rest of NO_3^- solution was sprayed sequentially onto each layer after packing. The incubation of such repacked soils instead of intact soil columns was chosen to i) systematically investigate the effect of aggregate size and to ii) guarantee thorough mixing of the ^{15}N tracer with the soil.

~~Packing in five vertical intervals achieved a uniform porosity across the column. However, there were inevitable porosity gradients within intervals (Figure S4) that affected the air and water distribution and thus air continuity at high water saturations. Three different saturation treatments were prepared for subsequent incubation experiments: 70%, 83% and 95% WHC. For the latter two saturation levels additional NO_3^- solution was sprayed sequentially onto each layer after packing.~~ In this way, a full factorial design with twelve treatments and three factors (soil: RM, GI; aggregate size: large, small; saturation: 70, 83, 95 % WHC) were prepared in triplicates for incubation. WHC was additionally measured for both soil materials in parallel soil cores. For a better comparability with previous studies the results will be presented in terms of water-filled pore space (WFPS), which is derived from the known mass of soil and water and their respective densities. A detailed description of the experimental setup can be found in the Supplementary Material.

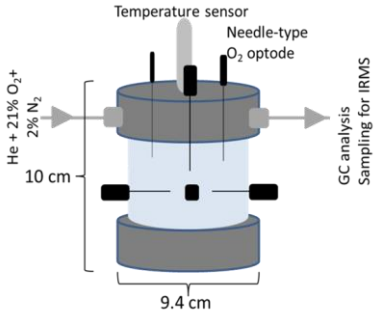

Figure 1: Schematic of the column for repacked soil showing the dimension (10 x 9.4 cm), the lid with in- and outlet for technical gas (21 % O_2 and 2 % N_2 in helium), in black O_2 microsensors and in gray the temperature sensor located in soil core.

The columns containing the packed soil aggregates were closed tightly and were equipped with an in- and outlet in the headspace (Figure 1). To analyse O_2 saturation, needle-type (40x0.8 mm) oxygen microsensors with <140 µm flat-broken sensor tip (NFSG-PSt1, PreSens Precision Sensing GmbH, Regensburg, Germany) were pinched through sealed holes in the lid and PVC column at seven well defined positions. Three sensors were located at the top by inserting vertically into the soil through the lid and headspace down to approximately 20 mm depth, whereas four sensors were inserted laterally at the centre of the column in about 36 mm depth with angular intervals of 90°. The microsensors were coupled to a multi-channel oxygen meter (OXY-10 micro, PreSens Precision Sensing GmbH, Regensburg, Germany) and O_2 measurements were stored in 15min intervals. The O_2 data were aggregated to 6 hour means for further analysis. The columns were placed in a darkened, temperature-controlled 20°C water bath (JULABO GmbH, Seelbach, Germany). Two flow controllers (G040, Brooks® Instrument, Dresden, Germany) served to flush the columns with technical gas (21% O_2 and 2% N_2 in helium, Praxair, Düsseldorf, Germany) through the inlet of the columns at a rate of 5 ml min^{-1}. This artificial atmosphere with low N_2 background concentration was used to increase sensitivity for N_2 fluxes (Lewicka-Szczebak et al., 2017). Initially, the headspace was flushed with technical gas for approximately 3 to 5 hours under 6 cycles of mild vacuum (max. 300mbar) to bring down the N_2 concentration within the soil column approximately to that of the technical gas (2%) and to ensure comparable initial conditions for incubation. Incubation time was 192 hours. Additional information on a parallel incubation where atmospheric conditions were switched from oxic to anoxic conditions to calculate the anaerobic soil volume fraction ($ansvf_{cal}$) can be found in the Supplementary Material.

2.2 Gas analysis

Gas chromatography (GC)

The columns outlet was directly connected to a gas chromatograph (Shimadzu 14B) equipped with an electron capture detector (ECD) to analyse N_2O and two flame ionization detectors (FID) to analyse methane (not reported) and CO_2. GC measurements were taken on-line every 6.5 minutes using GC Solution Software (Shimadzu, GCSolution 2.40). The detection limit was 0.25ppm N_2O and 261.90ppm CO_2 with a precision of at least 2 and 1%, respectively. The N_2O and CO_2 data were aggregated to 6 hour means for further analysis in order to eliminate the high frequency noise from the otherwise gradually changing gas concentrations under static incubation conditions. The measurements during an equilibration phase of 24h were excluded. N_2O fluxes derived from GC analysis may include N_2O from other processes than denitrification and is thus referred as the total net N_2O fluxes (N_2O_total).

Isotopic analysis

Samples for isotopic analysis of ^{15}N in N_2O and N_2 were taken manually after 1, 2, 4, and 8 days of incubation in 12 ml exetainers (Labco ©Exetainer, Labco Limited, Lampeter, UK). To elute residual air from the 12 ml exetainer it was flushed three times with helium (helium 6.0, Praxair, Düsseldorf, Germany) prior evacuating the air to 180 mbar. The exetainers were flushed with headspace gas for 15min, which amounts to a six-fold gas exchange of the exetainer volume. At the end of the incubation, technical gas was also sampled to analyze the isotopic signature of the carrier gas.

These gas samples were analysed using an automated gas preparation and introduction system (GasBench II, Thermo Fisher Scientific, Bremen, Germany, modified according to Lewicka-Szczebak et al. (2013) coupled to an isotope ratio mass spectrometer (MAT 253, Thermo Fisher Scientific, Bremen, Germany) that measured m/z 28 ($^{14}N^{14}N$), 29 ($^{14}N^{15}N$), and 30 ($^{15}N^{15}N$) of N_2 and simultaneously isotope ratios of ^{29}R ($^{29}N_2/^{28}N_2$) and ^{30}R ($^{30}N_2/^{28}N_2$). All three gas species (N_2O, (N_2O+N_2), and N_2) were analysed as N_2 gas after N_2O reduction in a Cu oven. Details of measurement and calculations for fractions of different pools (i.e. N in N_2O (fp_N_2O) or N_2 (fp_N_2) originating from ^{15}N-labelled NO_3^- pool) were described elsewhere and are provided in Supplementary Material (Supplementary Material, Figure S3) (Spott et al., 2006; Lewicka-Szczebak et al., 2013; Buchen et al., 2016).

The product ratio (pr) [$N_2O/(N_2O+N_2)$] was calculated for each sample:

$$pr\ [-] = \frac{fp\_N_2O}{fp\_N_2O + fp\_N_2} \quad (1)$$

The calculated average pr [$N_2O/(N_2O+N_2)$] of each treatment was also used to calculate the average total denitrification fluxes (N_2O+ N_2 fluxes) during the incubation:

$$(N_2O + N_2)\ \left[\mu g\ N\ h^{-1} kg^{-1}\right] = \frac{N_2O\_total}{pr} \quad (2)$$

2.3 Microstructure analysis

Due to the experimental setup, it was only possible to scan the soil cores with X-ray CT (X-tek XTH 225, Nikon Metrology) once d~~D~~irectly after the incubation experiment ~~the soil cores were scanned with X-ray CT (X-tek XTH 225, Nikon Metrology)~~. The temperature sensor was removed, but the oxygen micro-sensors remained in place during scanning. The scan settings (190 kV, 330 µA, 708 ms exposure time, 1.5 mm Cu filter, 2800 projections, 2 frames per projection) were kept constant for all soils and saturations. The projections were reconstructed into a 3D tomogram with 8-bit precision and a spatial resolution of 60 µm using the filtered back projection algorithm in X-tek CT-Pro. Only macropores twice this nominal resolution were clear~~a~~ly detectable in the soil core images. Hence, at the lowest water saturation not all air-filled pores can be resolved, which will be discussed below. The 3D images were processed with the Fiji bundle for ImageJ (Schindelin et al., 2012) and associated plugins.

The raw data were filtered with a 2D non-local means filter for noise removal. A radial and vertical drift in grayscale intensities had to be removed (Iassonov and Tuller, 2010; Schlüter et al., 2016) before these corrected gray-scale images (Figure 2a) were segmented into multiple material classes using the histogram-based thresholding methods (Schlüter et al., 2014). The number of materials varied between two (air-filled pores, soil matrix) and four (air-filled pores, water-filled pores, soil matrix, mineral grains) depending on saturation and soil material. By means of Connected Components Labeling implemented in the MorpholibJ plugin (Legland et al., 2016) the air-filled pore space was further segmented into isolated and connected air-filled porosity, depending on whether there was a continuous path to the headspace (Figure 2b). Average oxygen supply in the core was estimated by three metrics: 1) Visible air-filled porosity (ε_{vis}) and connected air content (ε_{con}) determined by voxel counting (Figure 2b), 2) average air distance derived from the histogram of the Euclidean distances between all non-air voxels and their closest connected air voxel (Figure 2c,d) (Schlüter et al., 2019) and 3) the *ansvf* which corresponds to the volume fraction of air distance larger than a certain threshold. Therefore, in a sensitivity test, air distance thresholds of 0.6, 1.3, 2.5, 3.8 and 5.0 mm were used to estimate the *ansvf* and to find the best correlation between *ansvf* and N_2O as well as (N_2O+N_2) fluxes. This was found with an *ansvf* at a critical air distance of 5 mm when pooling GI and RM soils (Figure 2c,d).

In summary, the ε_{con} is a proxy for the supply with gaseous oxygen coming from the headspace, whereas the connected air distance and *ansvf* are proxies for the supply limitation of dissolved oxygen by diffusive flux through the wet soil matrix. In addition to these averages for entire soil cores, both ε_{con} and average air distance were also computed locally in the vicinity of oxygen sensor tips (Figure 2b-c), to compare these metrics with measured oxygen concentrations. Spherical regions of interest (ROI) with different diameters from 3.6 to 10.8 mm were tested with respect to highest correlation of ε_{con} and average air distance with average oxygen concentration of individual sensors. This was found to occur at a diameter of 7.2 mm, when centered on the sensor tip.

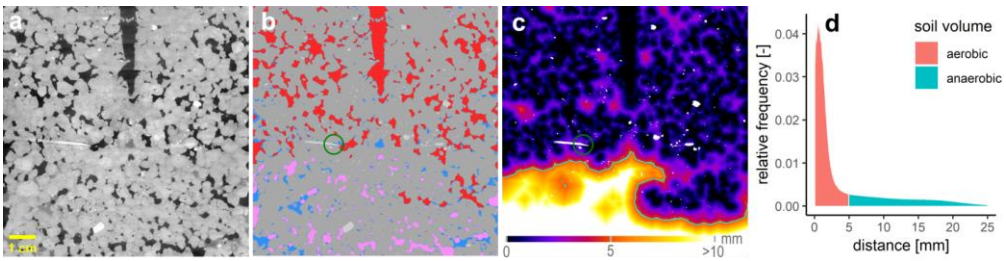

Figure 2: (a) 2D slice of packed GI soil with large aggregates and 75% WFPS. One oxygen microsensor is shown on the left and the hole of the temperature sensor at the top. (b) Material classes including soil matrix (gray), water (blue), mineral grains (light gray), connected air (red) and isolated air (rose). The green circle around the sensor tip depicts the diameter of 7.2 mm that is used to characterize its environment. (c) Euclidean distance to the closest connected air voxels (mineral grains are excluded). The green line depicts the connected air distance threshold of 5 mm that differentiates between an anaerobic soil volume fraction (light colors) or aerated volume. (d) Relative frequency of soil volume as a function of distance to closest connected air [mm] divided into aerobic (red) and anaerobic (green).

In addition to scans of the entire core, four individual aggregates (4-8 mm) of each soil were also scanned with X-ray CT (80 kv, 75 µA, 1s exposure time, no filter, 2400 projections, 2 frames per projection), reconstructed in 8-bit at a voxel resolution of 5 µm, filtered with a 2D non-local means filter and segmented into pores and background with the Otsu thresholding method (Otsu, 1975). The largest cuboid fully inscribed in an aggregate was cut and used for subsequent diffusion modelling as described below.

2.4 Diffusivity simulations

Diffusivity was simulated for individual aggregates as well as for the entire soil core (bulk diffusivity) directly on segmented X-ray CT data by solving the Laplace equation with the DiffuDict module in the GeoDict 2019 Software (Math2Market GmbH, Kaiserslautern, Germany). A hierarchical approach was used to (1) estimate the effective diffusivity of the wet soil matrix by simulating Laplace diffusion on individual soil aggregates with the Explicit Jump solver (Wiegmann and Bube, 2000; Wiegmann and Zemitis, 2006) and (2) model diffusivity (D_{sim}) with the Explicit Jump solver on the entire soil core (1550x1550x[1500-1600] voxels). The latter was based on the visible 3D pore space and using the effective diffusion coefficient of the soil matrix as obtained from the simulation of soil aggregates. We assumed an impermeable exterior, impermeable mineral grains (GI only) and the diffusion coefficient of oxygen in air and water (≥75%WFPS only) in the respective material classes (see detailed information in Supplementary Material).

2.5 Statistical analysis

Statistical analysis was conducted with R (R Core Team, 2018). Figures were produced with package ggplot2 (Wickham, 2016). In order to estimate the correlation between various variables that do not exhibit a normal distribution (average values of N_2O fluxes, (N_2O+N_2) fluxes, CO_2 fluxes, O_2 saturation, D_{sim}, ε_{con}, *ansvf* and *pr*) Spearman's rank correlations with pairwise deletion of missing values was performed pooling data for GI and RM soils. The p-values were corrected for multiple comparison according to Benjamini and Hochberg (1995) and adjusted p-values $\leq$0.05 were considered as significant.

As described before, there were four missing values for *pr* due to limitation of the isotopic measurement at the lowest saturation. For further statistical analysis of the dataset, any missing *pr* values were imputed using the chained random forest using more than 100 regression trees, in terms of overall variable pattern, as this method can handle nonlinear relationships between variables (Breiman, 2001; Nengsih et al., 2019). It was also required to standardize the data of very different value ranges for further analysis. Since N_2O and/or (N_2O+N_2) were not detectable for a few samples at the lowest saturation, a constant of 1 was added to N_2O and (N_2O+N_2) fluxes prior transformation. This changes the mean value but not the variance of data. In order to get normal distributions and linear relationships, a logarithmic transformation was applied to metric data (CO_2, N_2O and (N_2O+N_2) fluxes, D_{sim}), whereas a logistic transform $\mathrm{logit}(x) = \log(x/(1-x))$ was applied to dimensionless ratios between 0 and 1 (*ansvf*).

Since there was a high collinearity among most variables, a partial least square regression (PLSR) with Leave-One-Out Cross-validated R^2 was the best method to identify the most important independent explanatory variables (six predictors: CO_2 fluxes, O_2 saturation, D_{sim}, ε_{con}, *ansvf* and *pr*) to predict the response variables N_2O or (N_2O+N_2) fluxes. It has to be emphasized that N_2O fluxes and *pr* were measured independently of each other using different measuring methods (gas chromatography and isotopic analysis) what justifies *pr* as a predictor variable for N_2O fluxes. In contrast to this (N_2O+N_2) fluxes were calculated from *pr* and therefore *pr* was not included in PLSR for the response variable (N_2O+N_2) fluxes (resulting in five explanatory variables). Bootstrapping was used to provide confidence intervals that are robust against deviations from normality (R package boot v. 1.3-24) (Davison and Hinkley, 1997; Canty and Ripley, 2019). Given the relatively small sample size (36 incubations in total), the smoothed bootstrap was used by resampling from multivariate kernel density (R package kernelboot v. 0.1.7) (Wolodzko, 2020). The BCa bootstrap confidence interval of 95% of R^2 was a measure to explain the variability in each response variable (Efron, 1987). Components that best explained N_2O and (N_2O+N_2) fluxes were identified by permutation testing.

To address the second research question of this study concerning substitutions of predictors by classical, averaged soil properties additional and simplified models with the PLSR approach described above were performed using various variables to

substitute most important predictors for N_2O or (N_2O+N_2) fluxes. A detailed description of the substitution is provided in the result section 3.4 and discussion section 4.2.

3 Results

3.1 Bulk respiration

Time series of CO_2 and N_2O fluxes (Supplementary Material, Figure S1) show aggregated values for six hour steps over the complete incubation time of approximately 192 hours, ignoring the first 24 hours due to initial equilibration of the system (i.e. redistribution of water, expression of all denitrification enzymes, fast mineralization of labile carbon). Averages for the whole incubation are reported in Figure 3a, 3c and in Supplementary Material, Table S1, Table S2. The 3.7 times higher SOM content in GI soil than in RM soil resulted in higher microbial activity so that CO_2 fluxes were approximately ~~3~~ three times higher, for all saturations. The variability in CO_2 fluxes between replicates is much higher than the temporal variability during incubation. This is probably explained by small differences in packing of the columns that can have large consequences for soil aeration. CO_2 production in both soils was lowest with highest water saturation ~~(Figure 3a)~~ but were quite similar for both treatments with saturations <80% WFPS (Figure 3a). Aggregate size had a negligible effect on CO_2 production.

Substantial N_2O and (N_2O+N_2) emissions were detected for saturations ≥75% WFPS and were again approximately three times higher in SOM-rich GI soil than in RM soil (Figure 3c,~~-~~d). The variability between replicates is again higher than the temporal variability (e.g. in Figure 3d and time series in Supplementary Material, Figure S1) and the effect of aggregate size is inconsistent due to the large variability among replicates. Mineral N was not analyzed after the incubation and therefore cumulative (N_2O+N_2) fluxes were used to estimate the N loss after 192h of incubation. Considering the N addition of 50 mg N kg^{-1} as NO_3^- and an average natural NO_3^- background of 34 mg kg^{-1} substantial N loss was observed for both soils at ≥75% WFPS. ~~In RM soil t~~The N converted to N_2O or N_2 represents a proportion equal to ≤2.6% ~~2-4%~~ with RM soil and ≤8.0% with GI soil for both aggregate sizes and saturations. ~~With GI soil incubated at 75% WFPS the N loss was on average 5-11% for both aggregate sizes, whereas it reached 14% at 85% WFPS~~.

Average O_2 saturation was lowest with highest water saturation and roughly the same for saturations <80% WFPS (Figure 3b). Some sensors showed a gradual decline in O_2 concentration, whereas some showed a drastic reduction or increase in a short period of time, probably due to water redistribution (Supplementary Material, Figure S2). The average of the final 24h was taken for all subsequent analysis, as this probably best reflects the water distribution scanned with X-ray CT. Standard errors among the seven O_2 microsensors were high in each treatment due to very local measurement of O_2 that probed very different locations in the heterogeneous pore structure.

The *pr*, i.e. the $N_2O/(N_2O+N_2)$ as a measure of denitrification completeness, showed a similar behavior as a function of water saturation like N_2O release with a plateau for saturations ≥75% WFPS at 0.6 and a lower, but somewhat more erratic *pr* for the lowest saturation due to a generally low ^{15}N gas release (Figure 3e). Thus, the (N_2O+N_2) fluxes at ≤65% WFPS could only be calculated for a small number of samples, due to lacking data of *pr* (Supplementary Material, Table S1, Table S4). SOM content and aggregate size had no effect on *pr*. Time series of *pr* showed a gradual reduction for all treatments as the N_2 emissions grew faster than the N_2O emissions (Supplementary Material, Figure S5). With water saturations >75% WFPS the *pr* decreased with time and was in most cases <0.5 at the end of incubation (Supplementary Material, Figure S5). In summary, for each soil all samples with saturation ≥75% WFPS showed similar *pr* (Figure 3e) and N_2O release (Figure 3c). This agreed well with subsequent X-ray CT estimates of air connectivity as shown below.

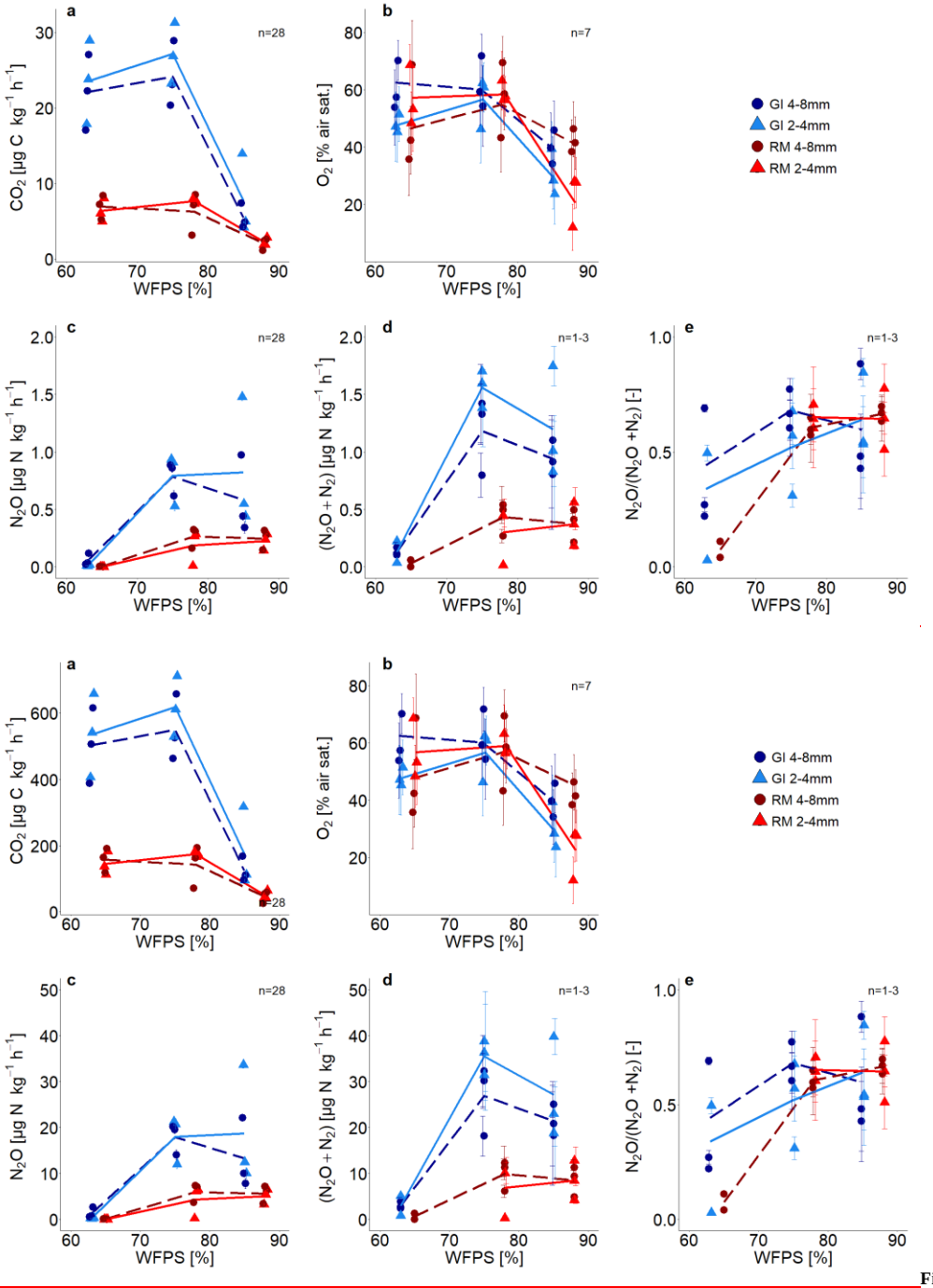

Figure 3: (a) Average CO_2 fluxes, (b) average O_2 saturation, (c) average N_2O and (d) (N_2O+ N_2) fluxes and (e) average product ratio (*pr*) [$N_2O/(N_2O+N_2)$] as a function of water saturation for soil from Rotthalmünster (RM) and Gießen (GI) and two aggregate sizes (2-4 and 4-8 mm). Symbols depict the average values for each of three individual replicates with error bars showing the standard error of the mean; standard error in (a) and (c) of fluxes measured during incubation, in (b) the standard error from measurements of seven

sensors located within the soil core and in (d) and (e) of three measurements during incubation time (after 2, 4, and 8 days with detectable R^{29} and R^{30}; n= 3 for two highest WFPS). The lines (dashed and solid) connect the average value of three replicates at each saturation (large and small aggregates, respectively).

3.2 Pore system of soil cores

Due to lower target bulk density in GI soil (1.0 g cm^{-3}) compared to that of RM soil (1.3 g cm^{-3}) visible air content (ε_{vis}, depicted in red and pink in Figure 2c) was higher independent of aggregate size (Figure 4a). The ε_{vis} decreased with increasing water saturation, but not linearly as would be expected. The air contents in the very wet range are in fact higher (16-17%), than the target air saturation of approximately 11 or 15% for RM and GI soil, respectively. It was not possible to remove air more efficiently during packing and some ponding water might have accidentally been removed with vacuum application during purging at the beginning of incubation. Additionally, the GI soil was rich in vermiculite and swelled upon wetting. This increase in soil volume at the end of incubation resulted in a relative decline in water content. For increasing water content the air content that is connected to the headspace (ε_{con}, depicted in red in Figure 2c) was reduced much more strongly as compared to the total ε_{vis}. This was observed for both soils and aggregate sizes and indicates that, a substantial amount of air is trapped (Figure 4b). According to this observation, average distance to visible air was very small (Figure 4c) and remained below 1.5 mm even for the highest water saturation with generally smaller distances for smaller aggregates. Yet, the average distance to the pore system connected with headspace escalates in the wet range (Figure 4d) ~~which results in an *ansvf* of 50-90% (Figure 4f)~~. The huge variability among replicates comes from the fact that trapping by complete water blockage typically occurs in the slightly compacted upper part of a packing interval, but the specific interval where this happens varies among samples (Supplementary Material, Figure S4). The different aggregate sizes did not affect the distance to connected air as the long-range continuity of air is controlled by bottle-necks in the pore space and not by aggregate size.

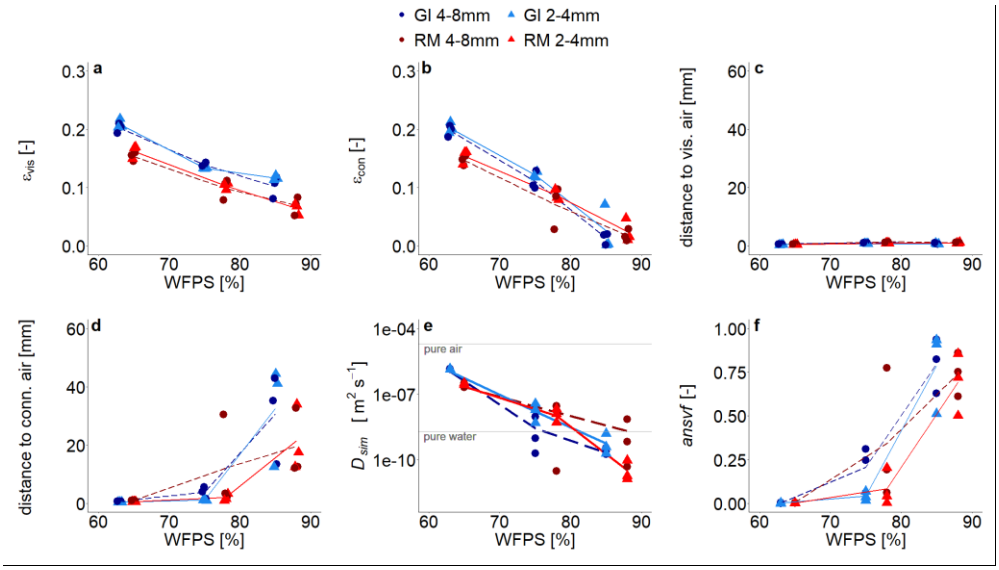

Figure 4: (a) Visible air content (ε_{vis}), (b) connected air content (ε_{con}), (c) average distance to visible air, (d) average distance to connected visible air, (e) simulated diffusivity (D_{sim}) and (f) anaerobic soil volume fraction (*ansvf*) as a function of water saturation for soil from Rotthalmünster (RM) and Gießen (GI), two aggregate sizes (2-4 and 4-8 mm) and three replicates each depicted by symbols. The lines (dashed and solid) connect the average value of three replicates (large and small aggregates, respectively). The horizontal gray lines in (e) reflect material properties. The experiment was performed at 20°C and according to that diffusivity was calculated at 20°C.

Water saturation had a dramatic impact on D_{sim} (Figure 4e) leading to a reduction by five orders of magnitude in a rather small saturation range. At high saturations it fell below the oxygen diffusion coefficient in pure water due to the tortuosity of the pore system. The *ansvf* (Figure 4f) is directly linked to connected air distance and shows the same escalating behavior at the highest saturation up to a volume fraction of 50-90%. The *ansvf* is highly correlated with CO_2 emissions (Spearman's R>-0.7 and p=0.04) which exhibits the same tipping point behavior, yet with very different slopes in the regression for the different soils due to different microbial activity (Figure S6). The correlation of *ansvf* is weaker with N_2O (Spearman's 0.6<R<0.77, p<0.1) and negligible with (N_2O+N_2) (p>0.2), suggesting that denitrification is more complexly controlled. The full regression analysis of *ansvf* with different gases and for different soils and aggregate sizes is presented in the supporting information (Figure S6).

~~The correlation of *ansvf* with average gas fluxes and internal O_2 concentrations is shown in Figure 5. Since the drop in CO_2 release at the highest water saturations coincided with an escalating *ansvf*, the relation between the two was highly correlated (Spearman's R> 0.7 and p=0.04) for all soils and aggregate sizes (Figure 5a), but with different slopes for both soils due to vastly different SOM contents. The correlation of *ansvf* with N_2O is weaker (Spearman's 0.6<R<0.77) and on the verge of being significant (p≤0.1) (Figure 5c). However, the correlation of *ansvf* with (N_2O+N_2) release is even worse (p>0.2), so the mechanisms that govern N_2O and (N_2O+N_2) release must be more complex (Figure 5c, d). As expected the average O_2 saturation decreases with increasing *ansvf* (Figure 5b). Yet, correlation is lower than for CO_2 (Spearman's 0.6<R< 0.2, but p>0.2), likely due to limited representativeness of average O_2 concentrations derived from a few point measurements.~~

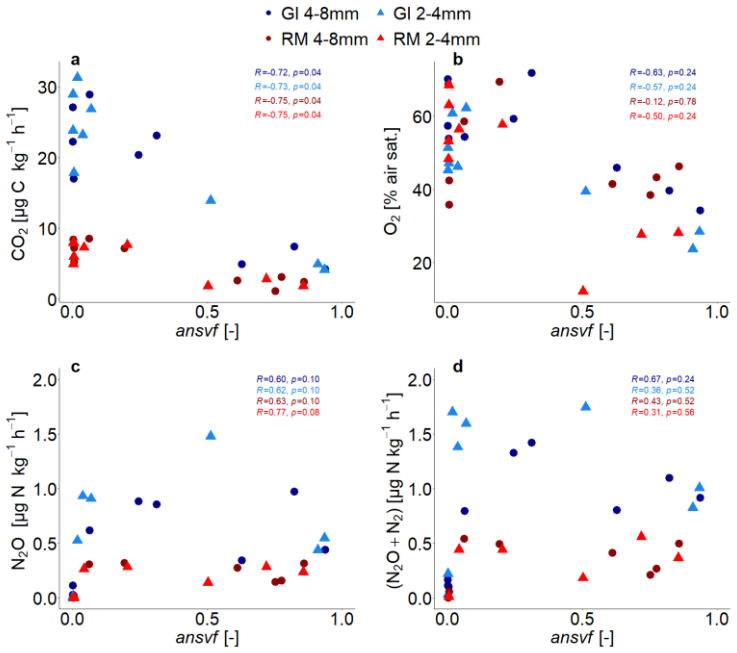

~~**Figure 5: Average (a) CO_2, fluxes (b) O_2 saturation, (c) N_2O and (d) (N_2O+N_2) fluxes as a function of anaerobic soil volume fraction (*ansvf*) for soil from Rotthalmünster (RM) and Gießen (GI) and two aggregate sizes (2-4 and 4-8 mm) for three individual replicates. The Spearman's rank correlation coefficient (*R*) result from Spearman's rank correlation and indicate the extent of monotonic relation between the ranks of both variables. The associated p-values (*p*) were corrected for multiple comparison according to Benjamini and Hochberg (1995).**~~

3.3 Microscopic oxygen distribution

The local measurements of O_2 using microsensors is demonstrated as an example for two selected sensors from the same soil column (GI soil incubated at 75% WFPS). They are located in the same depth with a separation distance of <2 cm. Sensor 1 detected low O_2 concentrations (18% air saturation) because it was located in a compact area with low ε_{con} (4%) and a rather large distance to the closest air-filled pore (1.6 mm) (Figure ~~6a~~5a,b,d). Sensor 2 detected fairly high O_2 concentrations (76% air saturation) as it happened to pinch into a macropore with a high ε_{con} (15%) and a short distance to connected air (0.8 mm) in its vicinity (Figure ~~6a~~5a-c). The green or violet circle with a diameter of 7.2 mm depicts the spherical averaging volume for ε_{con} and distance to connected air that correlated best with the average O_2 concentrations when lumped over all soils and saturations (Figure ~~6b~~5b-d).

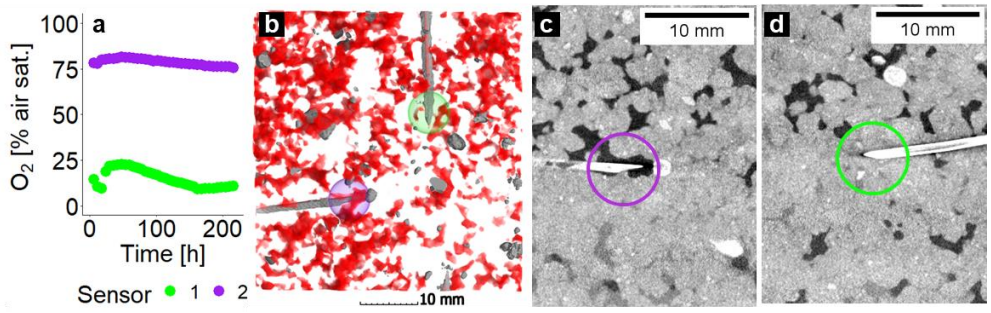

Figure ~~6~~5: Local oxygen distribution in one soil core packed with small aggregates (2-4 mm) from Gießen soil (GI) incubated at 75% WFPS to illustrate as an example the very local measurement of O_2. Shown here are (a) O_2 saturations measured by two microsensors as a function of incubation time, (b) a 3D subvolume showing both sensors (connected air is depicted in red), and 2D images of the corresponding sensor tips (c) the sensor measuring high and (d) the sensor measuring low O_2 saturations. The violet or green circles depict the proximity of the sensor tip (7.2 mm diameter) used to calculate the averaged local metrics.

The treatment specific correlations between distance to connected air and average O_2 concentrations are shown in Figure ~~7~~6. At the lowest saturation level there is no correlation at all (Spearman's $-0.4<<R<0.1$ and $p \geq 0.38$, Figure ~~7a~~6a,d), because some unresolved pores (<120 µm) within the aggregates are air-filled so that oxygen availability is not limited by visible air. At the intermediate saturation level the correlations were best (Spearman's $R<-0.7$ and $p \leq 0.02$) because all unresolved pores are water-filled (Figure ~~7b~~6b,e). At the highest water saturation the correlation was highest for large aggregates (Spearman's $R=-0.6$ and $p=0.08$), because the local effect of soil structure might become stronger relative to the non-local effect of air entrapment. With the other three treatments the correlation were worse again (Spearman's R between -0.01 and -0.3 and $p \geq 0.58$, Figure ~~7c~~6c,f), because distance to connected air ignores all trapped air which may still contribute a lot to oxygen supply.

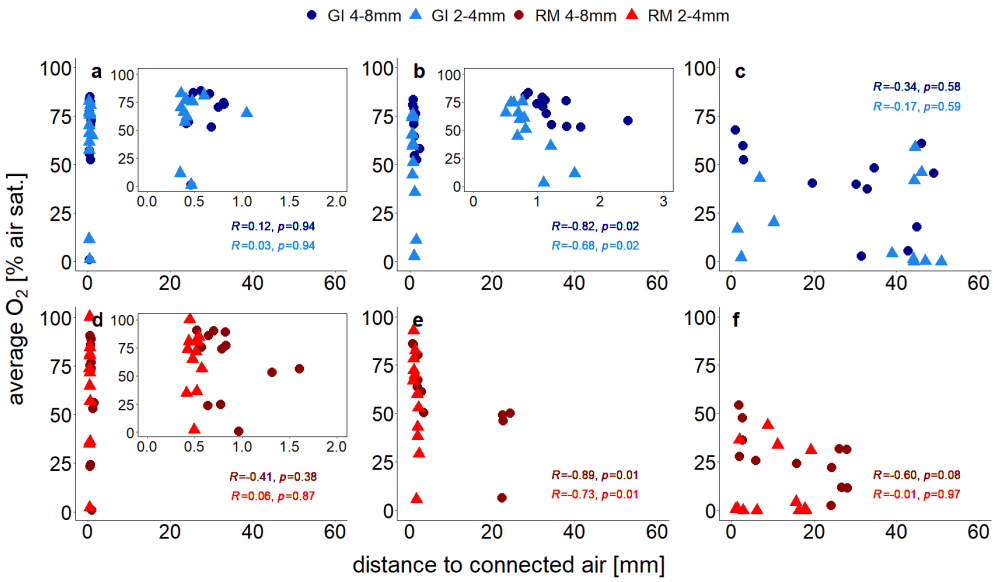

Figure ~~7~~6: Average O_2 saturation (at the end of incubation experiment) measured with 4 sensors each located at the center of soil core as a function of distance to visible connected air ~~regression~~ for soil from Gießen (GI, (a)-(c), blue) and Rotthalmünster (RM, (~~a~~d)-(~~c~~f), red) ~~and Gießen (GI, (d)-(f), blue)~~, and for two aggregate sizes (2-4 mm and 4-8 mm). (a) and (d) show results for lowest, (b) and (e) for medium, and (c) and (f) for highest water saturation. The inset in (a), (b), and (d) show~~s~~ a reduced distance range. The distance to visible connected air is averaged in a spherical region around the sensor tip (7.2 mm diameter). The Spearman's rank correlation coefficient (*R*) result from Spearman's rank correlation and indicate the extent of monotonic relation between the ranks of both variables. The associated p-values (*p*) were corrected for multiple comparison according to Benjamini and Hochberg (1995).

3.4 Explanatory variables for denitrification

So far the correlations among different explanatory variables and between explanatory variables and N-gas release have been shown for individual treatments, i.e. separately for each combination of soil and aggregate size, in order to focus on the effect of water saturation. However, the true potential of explanatory variables to predict denitrification can only be explored with the entire pooled data set, so that the variability in denitrification is captured more representatively.

The PLSR identified two principal components that best explained N_2O and N_2O+N_2 fluxes, while most variables contributed to the first component (Comp1) and almost exclusively CO_2 release contributed to the second component (Comp2) (see Supplementary Material ~~S7~~S8). These principal components revealed vastly different ability of individual explanatory variables to explain the observed variability in N_2O and (N_2O+N_2) release. The importance of explanatory variables to predict N_2O and N_2O+N_2 fluxes varied as follows: CO_2 > (*pr* >) *ansvf* > D_{sim} > ε_{con} > O_2 (see Supplementary Material Figure ~~S7~~S8). Hereinafter *pr* shown in brackets illustrates its contribution to PLSR analysis for N_2O fluxes only. The explanatory variability, expressed in the text as R^2*100 [%], was ~~71~~82% for N_2O fluxes and ~~79~~78% for N_2O+N_2 fluxes when considering the complex model with all explanatory variables (CO_2 flux, O_2 saturation, ε_{con}, D_{sim}, *ansvf* (and *pr*)) (Figure ~~8~~7). The resulting regression equations can be found in Supplementary Material (Equation ~~3-6~~7-8).

Starting from this complex model a series of simplifications and substitutions of explanatory variables was conducted to assess in how far the resulting loss in predictive power is acceptable. Reducing the number of explanatory variables to the most important variables resulted in CO_2 and *ansvf* for (N_2O+N_2) release (83% explained variability, simplified model in Figure 8). In other words, the combination of these two predictors (*ansvf* and CO_2) is crucial, as CO_2 release explains the different denitrification

rates between the two soils, whereas *ansvf* explains the differences within a soil due to different saturations. To predict N_2O emissions the simplified model with most important explanatory variables CO_2, *ansvf* and *pr* as a third predictor resulted in ~~71~~81% of explained variability (Figure 8). Average O_2 saturation could be omitted for its small correlation with N_2O or (N_2O+N_2) release in general, whereas ε_{con} and D_{sim} could be omitted because of the high correlation with *ansvf* (Supplementary Material, Figure ~~S6~~S7).

The regression equations with R^2 values and a confidence interval of 95% in square brackets resulting from PLSR with CO_2, *ansvf* (and *pr*) identified as most important explanatory variables to predict N_2O or (N_2O+N_2) fluxes of the present study for data after log- or logit transformation:

$$\log(N_2O) = 0.56\ \log(CO_2) + 0.63\ \mathrm{logit}(ansvf) + 0.67\ pr;\ R^2 = 0.81\ [0.67\text{-}0.89] \quad (3)$$

$$\log(N_2O + N_2) = 1.00\ \log(CO_2) + 1.40\ \mathrm{logit}(ansvf)\ ;\ R^2 = 0.83\ [0.71\text{-}0.90] \quad (4)$$

Various variables were used to substitute best predictors (CO_2 or *ansvf*) (Figure ~~8~~7) in PLSR. The substitution of CO_2 by SOM or *ansvf* by ε_t, D_{sim} or empirical diffusivity (D_{emp}) based on total porosity and air content (Deepagoda et al., 2011) is explained in the discussion section 4.2.

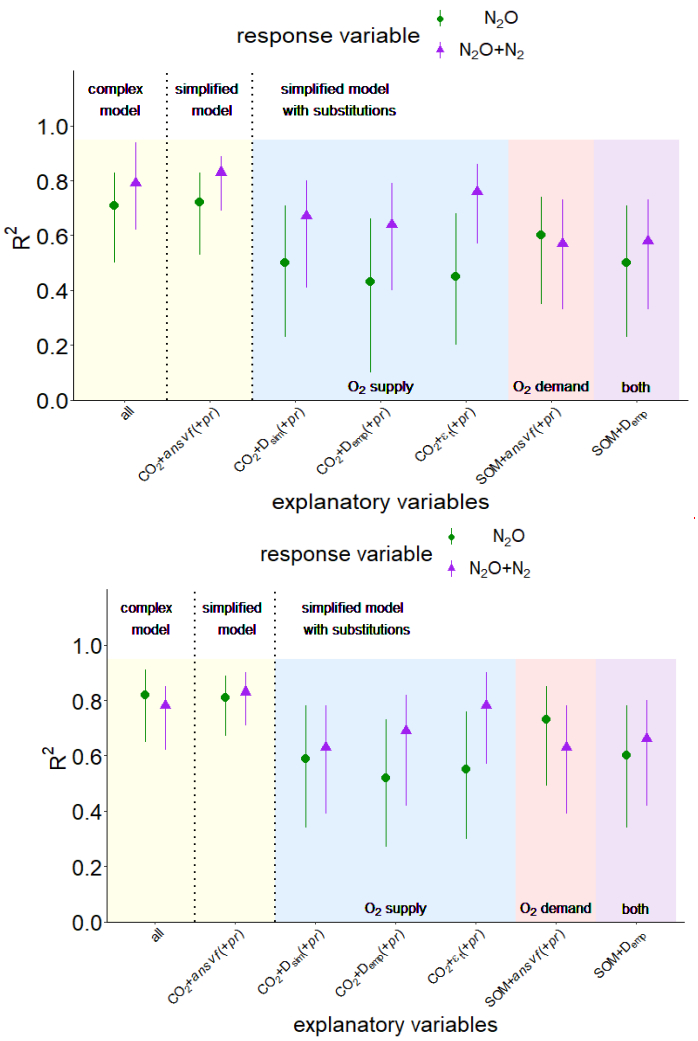

Figure ~~8~~7: Explained variability expressed as R^2 with a confidence interval of 95% resulting from partial least square regression (PLSR) with Leave-One-Out Cross-validation and bootstrapping for response variables N_2O (green symbols) or (N_2O+N_2) fluxes (violet symbols) for pooled data of both soils (RM and GI), WFPS treatments and aggregate sizes (n= 36). The yellow area shows a complex model including all explanatory variables of the present study (CO_2, O_2, connected air content (ε_{con}), diffusivity (D_{sim}), anaerobic soil volume fraction (*ansvf*), and product ratio (*pr*)) (all) and a simplified model included only most important predictors (*CO_2+ansvf(+pr)*). The blue area shows additional simplified models with substitutions of the most important predictor for O_2 supply (*ansvf*) by D_{sim} or diffusivity ~~from~~ calculated from an empirical model (D_{emp}) (Deepagoda et al., 2011), or theoretical air content (ε_t). The red area shows a simplified model with substitutions of the most important predictor for O_2 demand (CO_2) by SOM. Substitution of both most important predictors (CO_2 and *ansvf*) by SOM and D_{emp} is shown in the violet area.

4 Discussion

4.1 Which processes govern denitrification in soil?

The onset and magnitude of denitrification is controlled by O_2 supply and O_2 consumption, which in turn depends on processes in soil occurring at microscopic scales. This study was designed to examine different levels of O_2 consumptions by comparing soils with different SOM contents and different levels of O_2 supply by comparing different aggregate sizes and different water saturations. Other factors that would have affected O_2 demand and energy sources for denitrifiers (quality of organic matter, temperature, pH, plant-soil interactions), O_2 supply (oxygen concentration in the headspace, temperature) or other drivers of denitrification (NO_3^- concentration, pH, denitrifier community structure) were either controlled or excluded in this study.

N_2O release from soil can be low because denitrification does not occur under sufficient oxygen supply or because it is formed in wet soil but reduced to N_2 before it can escape to the atmosphere or because it is trapped in isolated air pockets (Braker and Conrad, 2011). Trapped N_2O is thought to likely be reduced to N_2 eventually if gaseous N_2O is not released after a saturation change, which would open up a continuous path to the headspace. This is shown in the schematic on the balance between O_2 supply and demand and its effect on denitrification (Figure ~~9~~8).

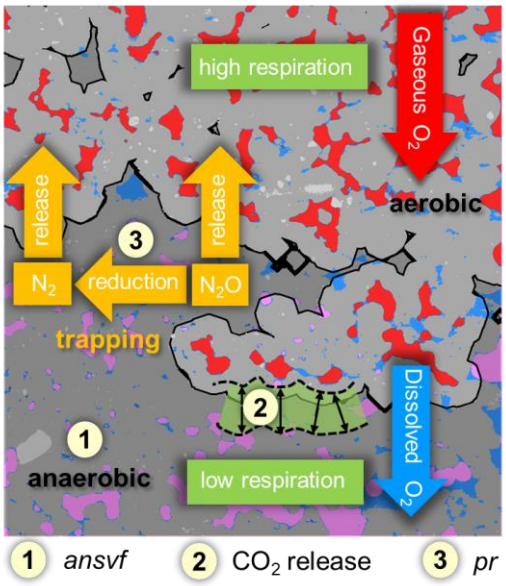

Figure ~~9~~8: Conceptual scheme of oxygen (O_2) supply and demand and its effect on denitrification. Material classes including soil matrix (gray area), water (blue), mineral grains (light gray), connected air (red) and isolated air (rose). The black line divides between aerobic (light gray area) and anaerobic (dark gray area) conditions. O_2 ~~Oxygen~~ supply and demand regulate the formation of anaerobic soil volume fraction (*ansvf*) as an imprint of the spatial distribution of connected air (item number 1), respiration (item number 2) that would move the boundary between oxic and anoxic zones in the soil matrix closer towards the pore when soil respiration is high (and vice versa) and N_2O reduction to N_2 (expressed by the product ratio (*pr*), item number 3). The numbered items show how the explanatory variables that best describe N_2O release affect denitrification.

To our knowledge, the experimental setup of the present study combined for the first time microstructure analysis of soil (X-ray CT) with measurements of N_2O and (N_2O+N_2) fluxes to explore controlling factors of the complete denitrification process including N_2 formation. The explanatory variables that contributed the highest predictive power with (N_2O+N_2) release were *ansvf* and CO_2 release (Figure ~~9~~8). The estimated *ansvf* (item 1) is a sole function of the spatial distribution of connected air in soil and therefore only reflects soil structural properties related to O_2 supply. The dependence of denitrification on diffusion

constraints was demonstrated by several models that were developed to predict the formation of anoxic centers within soil aggregates (Greenwood, 1961; Arah and Smith, 1989; Arah and Vinten, 1995; Kremen et al., 2005). The distance threshold for anoxic conditions to emerge was set on an ad-hoc basis at 5 mm from connected air at the end of incubation, but is likely to vary with O_2 demand by local microbial activity (CO_2 release represented by the green fringe area, item 2) during the incubation (Kremen et al., 2005; Rabot et al., 2015; Ebrahimi and Or, 2018; Keiluweit et al., 2018; Kravchenko et al., 2018; Schlüter et al., 2019). ~~-~~Because we could only conduct X-ray CT-scans at the end of incubation, redistribution of water during the incubation time cannot be ruled out. This could have changed *ansvf* and thus might explain some of the temporal variability of gaseous fluxes. In repacked soils it might be distributed rather uniformly and therefore correlated with bulk CO_2 release (Aon et al., 2001; Ryan and Law, 2005; Herbst et al., 2016). The fact that aggregate size had no effect on denitrification indicates that critical distances were larger than the aggregate radii and rather controlled by air distribution in the macropore system. This means that both ~~-~~aggregate sizes used in the present study might have been too small to provoke differences in CO_2, N_2O and (N_2O+N_2) fluxes. ~~This~~ The large distance found here is in contrast to the very short critical distances of 180 µm for sufficient soil aeration estimated by Kravchenko et al. (2018) and Kravchenko et al. (2019) for intact soil cores containing crop residues for which soil respiration was not determined but likely to be much higher.

A somewhat surprising result is that oxygen concentration measurements did not have an added value for predicting either N_2O release or total denitrification. Best correlation of local O_2 concentration with ε_{con} was with a radial extent of 3.6 mm used for averaging around the microsensor (Figure ~~7~~6). Thus, with seven microsensors per column we only probed 0.2% of the total soil volume. This is too small to capture aerobic and anaerobic conditions representatively, especially since they may switch within short distances (Figure ~~6~~5). More sensors or sensors with larger support volume could be a means to improve the predictive power of local oxygen measurements. However, there is always a trade-off between retrieving more information and disturbing the soil ~~is~~ as little as possible.

If only N_2O release is concerned, *pr* as an independent proxy for N_2O consumption (Figure ~~9~~ 8 (item 3)) was beneficial to predict N_2O emissions together with CO_2 and *ansvf* (Figure ~~8~~7). The N_2O reduction to N_2 and thus the *pr* are complexly controlled, where besides physical factors microbial (the structure of the denitrifier community) and chemical properties (pH, N oxides, SOM, temperature, salinity) are relevant (Smith et al., 2003; Clough et al., 2005; Müller and Clough, 2014). With respect to physical factors, decreasing diffusivity enhances N_2O residence time and N_2O concentration in the pore space thus favouring N_2O reduction. According to this, Bocking and Blyth (2018) assumed a very small *pr* in wet soils, because N_2O may be trapped in the soil or completely reduced to N_2. This assumption may also support results of the present study, where the average (N_2O+N_2) fluxes peaked at the medium water saturation (particularly with GI soil) while D_{sim} decreased with increasing water saturations (Figure 4), which may indicate an entrapment of (N_2O+N_2) in isolated soil pores (Clough et al., 2005; Harter et al., 2016). However, N_2 release increased more strongly with time than the N_2O release resulting in decreasing *pr* with time (Supplementary Material, Figure S5). The chance of N_2O to be released before it is reduced to N_2 depends on the diffusion distance of dissolved (and gaseous) N_2O between its formation sites and the atmosphere. Although diffusion pathways for O_2 and N_2O are similar just in opposite direction, *ansvf* and *pr* might be a good combination of proxies to predict N_2O emissions to capture physical and microbial properties.

4.2 How to substitute microscale information by bulk properties?

The aims of this study were to find a minimum set of variables that explain the regulation of microbial denitrification at microscopic scales in a simplified experimental setup and to explore in how far this microscopic information can be substituted by readily available bulk properties that are feasible to measure in a field campaign. The interplay of O_2 supply and ~~oxygen~~ O_2

demand resulted in CO_2 emissions and CT-derived *ansvf* being the most important predictors for (N_2O+N_2) fluxes, while for N_2O fluxes *pr* was also important (Figure ~~8~~7, see Supplementary Material Figure ~~S7~~S8S8). Simplified models with most important predictors only (*CO_2+ ansvf (+pr)*) were sufficient to achieve similar explained variabilities (~~71~~81% and 83% for N_2O and (N_2O+N_2) fluxes, respectively) compared to the complex models. The downside of using CO_2 and CT-derived *ansvf* as predictors for denitrification is that these proxies are often unavailable and reasonable substitutions by easily available variables would be desirable.

The *ansvf* could have been replaced with alternative proxies for O_2 supply like D_{sim}, D_{emp} and ε_t, which would have led to a reduction in explained variability of (N_2O+N_2) fluxes to ~~64-76~~52-78% and an even larger drop for N_2O fluxes to ~~43-50~~46-59% (Supplementary Material, Table S2~~, Figure S8S9~~). The substitution of *ansvf* by D_{sim} would avoid the requirement for an ad-hoc definition of a critical pore distance threshold but it is gained with the caveat of very time-consuming 3D simulations or laborious measurements. Therefore, the substitution of *ansvf* with diffusivity estimated by empirical models (D_{emp}) seems more viable. Diffusivity is mainly controlled by soil bulk density and water saturation (Balaine et al., 2013; Klefoth et al., 2014). These empirical models predict diffusivity based on empirical relationships with total porosity (Φ) and air-filled porosity (ε) (Millington and Quirk, 1961; Moldrup et al., 2000; Resurreccion et al., 2010; Deepagoda et al., 2011; Deepagoda et al., 2019). As expected the discrepancy between calculated D_{emp} and simulated D_{sim} was highest at water saturation >75% WFPS where discontinuity due to packing procedure took full effect as described earlier (Supplementary Material, Figure ~~S8~~S9, Figure S4). The substitution of CT-derived *ansvf* by D_{emp} derived from empirical models (Figure ~~8~~7, Supplementary Material, Table S2) is perhaps unacceptable for a genuine understanding of N_2O or (N_2O+N_2) emissions from individual samples since estimated diffusivity ignores the actual tortuosity and continuity of the air-filled pore space. However, it may be a promising approach to reasonably predict average N_2O or (N_2O+N_2) fluxes at natural conditions with readily available soil characteristics (Figure ~~8~~7, ~~Figure S6S7~~Table S2). In this particular study, D_{sim} could even be replaced with the theoretical air content (ε_t) adjusted during packing (together with CO_2*(+pr)*) without a reduction in explained variability in N_2O and (N_2O+N_2) fluxes (Figure ~~8~~7, Supplementary Material, Table S2), due to the very strong log-linear relationship between the ε_t and D_{sim} (Figure 4e). However, totally neglecting any proxy for O_2 supply, (i.e. CO_2 only to predict N_2O fluxes), was insufficient to predict N_2O fluxes (Table S2).

A different strategy to estimate *ansvf* from bulk measurements is to switch from oxic to anoxic incubation by replacing the carrier gas under otherwise constant conditions. The difference in (N_2O+N_2) release between the two stages will be larger, the smaller the *ansvf* during oxic incubation. Details about the calculation of this $ansvf_{cal}$ can be found in the Supplementary Material. The $ansvf_{cal}$ assumes that actual denitrification is linearly related to *ansvf* and that the specific anoxic denitrification rate is homogenous, i.e. would be identical at any location within the soil. Deviations from this assumption could arise from heterogeneity in the distribution of substrates and microbial communities. However, the actual soil volume where denitrification may occur, described by the distance to aerated pores, does not only depend on O_2 diffusion, but also on respiration (O_2 consumption). Therefore, it could be expected, that *ansvf* derived from X-ray CT imaging analysis compared to $ansvf_{cal}$ was overestimated with RM soil or underestimated with GI soil due to the differences in carbon sources and related O_2 consumption. The average $ansvf_{cal}$ was similar (0.~~20~~24) to the *ansvf* (0.21) for RM soil (Supplementary Material, Table S3). With GI soil, however, the $ansvf_{cal}$ was larger (0.~~38~~45) than the image-derived *ansvf* (0.13). This difference may indeed result from an underestimation of *ansvf* of GI soil due to the higher SOM content and respiration rates. In future experiments it might be recommendable to integrate the O_2 consumption into *ansvf* estimation. The appeal of this two-stage incubation is that it can be conducted with larger soil columns as there is no size restriction as with the application of X-ray CT. Evidently, this two-stage incubation approach is not feasible for field campaigns, for which we would recommend to resort to estimated diffusivities

instead. However, both approaches are complementary since both are associated with different assumptions and thus uncertainties. Therefore, using them both improves the assessment of *ansvf*.

The use of CO_2 production as a proxy for O_2 demand to predict N_2O and (N_2O+N_2) release is limited as it is not fully independent of denitrification, since anaerobic respiration contributes to total respiration. Therefore, it is appealing to replace it with estimates of microbial activity based on empirical relationships with temperature, SOM, clay and water content (Smith et al., 2003) as these properties are routinely measured. When including the SOM measured before the experiment for the bulk soil (Table 1) to explore N_2O or (N_2O+N_2) emissions, predictive power for (N_2O+N_2) decreased (~~57~~63% compared to 83% with CO_2 instead of SOM together with *ansvf*), just like it was reduced for predicting N_2O emissions (~~60~~73% compared to ~~71~~81% with CO_2 instead of SOM together with *ansvf* and *pr*). The combination of proxies for O_2 supply and demand, SOM and D_{emp} only, to predict N_2O and (N_2O+N_2) fluxes did not reduce the explained variability too much beyond those of individual substitutions (~~50~~ 60 and ~~58~~66%, respectively). An improvement might be achieved by accounting for different quality in SOM, e.g. mineral-associated organic matter, fresh particulate organic matter, microbial pool; all of which will lead to different mineralisation rates and hence propensity to run into local anoxia (Beauchamp et al., 1989; Kuzyakov, 2015; Surey et al., 2020), due to the fact that SOM favours denitrification in several ways (Beauchamp et al., 1989; Ussiri and Lal, 2013), i.e. by supplying energy, leading to consume O_2 via respiration and supplying mineral N from mineralisation. ~~Thus, in future studies the SOM content of bulk soil or more involved empirical models that account for temperature and other independent variables instead of values from the more laborious CO_2 measurement could be a promising variable to predict N_2O emissions together with variables describing the soil structure.~~

4.3 Future directions and implications for modeling

In large-scale effective N-cycling models the *ansvf* is typically linked to the partial pressure of oxygen in soil and conveys no explicit spatial information. In the long run these models like DNDC, CoupModel, MicNiT (Li et al., 1992; Jansson and Karlberg, 2011; Blagodatsky et al., 2011) might benefit tremendously from incorporating a spatially explicit *ansvf* as a state variable to predict denitrification. The estimation of *ansvf* can be improved by taking O_2 consumption into account. Knowledge on spatial distribution of respiration in combination with pore scale modeling would further improve *ansvf* estimations and could be used to validate our approach with oxic/anoxic incubation. However, the empirical functions to estimate this *ansvf* from readily available properties similar to empirical diffusivity models have yet to be developed and validated against a whole suite of intact soil cores with different soil types and vegetation for which oxic/anoxic incubation and X-ray CT analysis are carried out jointly.

Using intact instead of repacked soils in future experiments will represent more natural conditions, e.g. larger tortuosity and thus lower diffusivity in undisturbed compared to sieved soil (Moldrup et al., 2001). However, in undisturbed soils diffusivity and soil structure may also vary locally and as a consequence of this varying O_2 supply and demand affect denitrification. Under field conditions this impact on denitrification is additionally altered by saturation changes, temperature variations, atmospheric gas concentrations, microbial community structure, and plant growth. It would thus be very interesting to include also different soil types and land-use types from various climate zones in future studies, e.g. paddy soils having high water saturation and are known to show a high denitrification activity with N_2 emissions exceeding that of N_2O emissions.

Conclusions

To our knowledge this is the first experimental setup combining X-ray CT derived imaging and flux measurements of complete denitrification (i.e. N_2O and (N_2O+N_2) fluxes) to explore the microscopic drivers of denitrification in repacked soil. We could show that changes in denitrification within different saturations could be predicted well with the anaerobic soil volume fraction (*ansvf)* estimated from image-derived soil structural properties. The differences in denitrification (i.e. N_2O and (N_2O+N_2) fluxes) between two investigated soils were triggered by different respiration rates due to different SOM content. A combination of CT-derived *ansvf* and CO_2 emission, as proxies for oxygen supply and demand, respectively, is best in predicting (N_2O+N_2) emission (83% explained variability) across a large saturation range and two different soils. The product ratio (*pr)*, additionally to *ansvf* and CO_2 emissions, was also an important predictor for emissions of only the greenhouse gas N_2O (~~71~~81% explained variability). The *ansvf* can also be replaced by simulated diffusivity (D_{sim}) (time consuming) or by diffusivity from empirical models (D_{emp}) but not without losing predictive power. A replacement of CO_2 fluxes by SOM also resulted in lower predictive power, but is recommended for large-scale applications since SOM is an independent proxy for microbial activity. The full substitution of laborious predictors (*ansvf, pr,* CO_2) by readily available alternatives (SOM, D_{emp}) reduced the explained variability to ~~50~~ 60 and ~~58~~66% for N_2O and (N_2O+N_2) fluxes, respectively.

The high explanatory power of image-derived *ansvf* opens up new perspectives to make predictions (e. g. by modelling approaches or in pedo-transfer functions) from independent measurements of soil structure using new techniques (e.g. X-ray CT analysis) available today in combination with biotic properties, e. g. quantity or quality of SOM. This paves the way for explicitly accounting for changes in soil structure (e. g. tillage, plants) and climatic conditions (e. g. temperature, moisture) on denitrification.

Data availability. CT data and gas emission data are available from the authors on request.

Author contribution. H-JV, RW and SS designed the experiment. SS, BA and LR carried out the experiment. G-MW developed the statistical analysis. SS and LR prepared the manuscript with contributions from all co-authors.

Competing interests. The authors declare that they have no conflict of interest.

Acknowledgments. We thank Jürgen Böttcher from the Institute of Soil Science, Leibniz University in Hannover, for measurements of soil materials used for incubation and Anette Giesemann and Martina Heuer from Thünen-Institute for Climate-Smart Agriculture in Braunschweig, Germany, for isotopic analysis. Our thanks go to Ines Backwinkel und Jan-Reent Köster from Thünen-Institute for Climate-Smart Agriculture in Braunschweig, Germany, for conducting parallel incubations under oxic and anoxic conditions. This study is funded by the Deutsche Forschungsgemeinschaft through the research unit research unit DFG-FOR 2337: Denitrification in Agricultural Soils: Integrated Control and Modelling at Various Scales (DASIM), grant umber 270261188.

References

Andersen, A. J., and Petersen, S. O.: Effects of C and N availability and soil-water potential interactions on N_2O evolution and PLFA composition, Soil Biol. Biochem., 41, 1726-1733, https://doi.org/10.1016/j.soilbio.2009.06.001, 2009.

Aon, M. A., Sarena, D. E., Burgos, J. L., and Cortassa, S.: Interaction between gas exchange rates, physical and microbiologi cal properties in soils recently subjected to agriculture, Soil Tillage Res., 60, 163-171, https://doi.org/10.1016/S0167-1987(01)00191-X, 2001.

Arah, J. R. M., and Smith, K. A.: Steady-state denitrification in aggregated soil - A mathematical approach, Journal of Soil Science, 40, 139-149, https://doi.org/10.1111/j.1365-2389.1989.tb01262.x, 1989.

Arah, J. R. M., and Vinten, A. J. A.: Simplified models of anoxia and denitrification in aggregated and simple-structured soils, European Journal of Soil Science, 46, 507-517, https://doi.org/10.1111/j.1365-2389.1995.tb01347.x, 1995.

Balaine, N., Clough, T. J., Kelliher, F. M., and van Koten, C.: Soil aeration affects the degradation rate of the nitrification inhibitor dicyandiamide, Soil Research, 53, 137-143, https://doi.org/10.1071/SR14162, 2015.

Balaine, N., Clough, T. J., Beare, M. H., Thomas, S. M., and Meenken, E. D.: Soil gas diffusivity controls N_2O and N_2 emissions and their ratio, Soil Sc. Soc. Am. J., 80, 529-540, https://doi.org/10.2136/sssaj2015.09.0350, 2016.

Beauchamp, E. G., Trevors, J. T., and Paul, J. W.: Carbon sources for bacterial denitrification, in: Advances in Soil Science: Volume 10, edited by: Stewart, B. A., Springer New York, New York, NY, 113-142, 1989.

Benjamini, Y., and Hochberg, Y.: Controlling the false discovery rate: a practical and powerful approach to multiple testing, Journal of the Royal Statistical Society. Series B (Methodological), 57, 289-300, 1995.

Blagodatsky, S., Grote, R., Kiese, R., Werner, C., and Butterbach-Bahl, K.: Modelling of microbial carbon and nitrogen turnover in soil with special emphasis on N-trace gases emission, Plant and Soil, 346, 297-330, https://doi.org/10.1007/s11104-011-0821-z, 2011.

Bocking, C. R., and Blyth, M. G.: Oxygen uptake and denitrification in soil aggregates, Acta Mechanica, 229, 595-612, https://doi.org/10.1007/s00707-017-2042-x, 2018.

Braker, G., and Conrad, R.: Diversity, structure, and size of N_2O-producing microbial communities in soils-What matters for their functioning?, in: Advances in Applied Microbiology, Vol 75, edited by: Laskin, A. I., Sariaslani, S., and Gadd, G. M., Advances in Applied Microbiology, 33-70, 2011.

Breiman, L.: Random forests, Machine Learning, 45, 5-32, https://doi.org/10.1023/A:1010933404324, 2001.

Buchen, C., Lewicka-Szczebak, D., Fuß, R., Helfrich, M., Flessa, H., and Well, R.: Fluxes of N_2 and N_2O and contributing processes in summer after grassland renewal and grassland conversion to maize cropping on a Plaggic Anthrosol and a Histic Gleysol, Soil Biol. Biochem., 101, 6-19, http://dx.doi.org/10.1016/j.soilbio.2016.06.028, 2016.

Butterbach-Bahl, K., Baggs, E. M., Dannenmann, M., Kiese, R., and Zechmeister-Boltenstern, S.: Nitrous oxide emissions from soils: how well do we understand the processes and their controls?, Philosophical Transactions of the Royal Society B: Biological Sciences, 368, https://doi.org/10.1098/rstb.2013.0122, 2013.

Cabello, P., Roldán, M. D., and Moreno-Vivián, C.: Nitrate reduction and the nitrogen cycle in archaea, Microbiology, 150, 3527-3546, https://doi.org/10.1099/mic.0.27303-0, 2004.

Canty, A., and Ripley, B.: boot: Bootstrap R (S-Plus) Functions . R package version 1.3-24, 2019.

Clough, T. J., Sherlock, R. R., and Rolston, D. E.: A review of the movement and fate of N_2O in the subsoil, Nutrient Cycling in Agroecosystems, 72, 3-11, https://doi.org/10.1007/s10705-004-7349-z, 2005.

Davidson, E. A., Verchot, L. V., Cattânio, J. H., Ackerman, I. L., and Carvalho, J. E. M.: Effects of soil water content on soil respiration in forests and cattle pastures of eastern amazonia, Biogeochemistry, 48, 53-69, https://doi.org/10.1023/A:1006204113917, 2000.

Davison, A. C., and Hinkley, D. V.: Bootstrap methods and their application, Cambridge Series in Statistical and Probabilistic Mathematics, Cambridge University Press, Cambridge, 1997.

Deepagoda, T., Moldrup, P., Schjonning, P., de Jonge, L. W., Kawamoto, K., and Komatsu, T.: Density-corrected models for gas diffusivity and air permeability in unsaturated soil, Vadose Zone J., 10, 226-238, https://doi.org/10.2136/vzj2009.0137, 2011.

Deepagoda, T., Jayarathne, J., Clough, T. J., Thomas, S., and Elberling, B.: Soil-gas diffusivity and soil-moisture effects on N_2O emissions from intact pasture soils, Soil Sc. Soc. Am. J., 83, 1032-1043, https://doi.org/10.2136/sssaj2018.10.0405, 2019.

Ebrahimi, A., and Or, D.: Dynamics of soil biogeochemical gas emissions shaped by remolded aggregate sizes and carbon configurations under hydration cycles, Glob. Change Biol., 24, e378-e392, https://doi.org/10.1111/gcb.13938, 2018.

Efron, B.: Better bootstrap confidence intervals, Journal of the American Statistical Association, 82, 171-185, https://doi.org/10.2307/2289144, 1987.

Elberling, B., Askaer, L., Jørgensen, C. J., Joensen, H. P., Kühl, M., Glud, R. N., and Lauritsen, F. R.: Linking soil O_2, CO_2, and CH_4 concentrations in a wetland soil: implications for CO_2 and CH_4 fluxes, Environmental Science & Technology, 45, 3393-3399, https://doi.org/10.1021/es103540k, 2011.

Greenwood, D. J.: The effect of oxygen concentration on the decomposition of organic materials in soil, Plant and Soil, 14, 360-376, https://doi.org/10.1007/BF01666294, 1961.

Groffman, P. M., and Tiedje, J. M.: Denitrification hysteresis during wetting and drying cycles in soil, Soil Sci Soc Am J, 52, https://doi.org/10.2136/sssaj1988.03615995005200060022x, 1988.

Groffman, P. M., Altabet, M. A., Bohlke, J. K., Butterbach-Bahl, K., David, M. B., Firestone, M. K., Giblin, A. E., Kana, T. M., Nielsen, L. P., and Voytek, M. A.: Methods for measuring denitrification: Diverse approaches to a difficult problem, Ecological Applications, 16, 2091-2122, 2006.

Harter, J., Guzman-Bustamante, I., Kuehfuss, S., Ruser, R., Well, R., Spott, O., Kappler, A., and Behrens, S.: Gas entrapment and microbial N_2O reduction reduce N_2O emissions from a biochar-amended sandy clay loam soil, Scientific Reports, 6, 39574, https://doi.org/10.1038/srep39574 2016.

Hayatsu, M., Tago, K., and Saito, M.: Various players in the nitrogen cycle: Diversity and functions of the microorganisms involved in nitrification and denitrification, Soil Science & Plant Nutrition, 54, 33-45, https://doi.org/10.1111/j.1747-0765.2007.00195.x, 2008.

Herbst, M., Tappe, W., Kummer, S., and Vereecken, H.: The impact of sieving on heterotrophic respiration response to water content in loamy and sandy topsoils, Geoderma, 272, 73-82, https://doi.org/10.1016/j.geoderma.2016.03.002, 2016.

Højberg, O., Revsbech, N. P., and Tiedje, J. M.: Denitrification in soil aggregates analyzed with microsensors for nitrous oxide and oxygen, Soil Sc. Soc. Am. J., 58, 1691-1698, https://doi.org/10.2136/sssaj1994.03615995005800060016x, 1994.

Iassonov, P., and Tuller, M.: Application of segmentation for correction of intensity bias in X-ray computed tomography images, Vadose Zone Journal, 9, 187-191, 2010.

Jäger, H. J., Schmidt, S. W., Kammann, C., Grunhage, L., Muller, C., and Hanewald, K.: The University of Giessen Free-Air Carbon dioxide Enrichment study: Description of the experimental site and of a new enrichment system, J. Appl. Bot.-Angew. Bot., 77, 117-127, 2003.

Jansson, P.-E., and Karlberg, L.: COUP Manual: Coupled heat and mass transfer model for soil-plant-atmosphere systems, https://www.coupmodel.com/documentation, 2011.

John, B., Yamashita, T., Ludwig, B., and Flessa, H.: Storage of organic carbon in aggregate and density fractions of silty soils under different types of land use, Geoderma, 128, 63-79, https://doi.org/10.1016/j.geoderma.2004.12.013, 2005.

Jones, C. M., Stres, B., Rosenquist, M., and Hallin, S.: Phylogenetic analysis of nitrite, nitric oxide, and nitrous oxide respiratory enzymes reveal a complex evolutionary history for denitrification, Mol. Biol. Evol., 25, 1955-1966, https://doi.org/10.1093/molbev/msn146, 2008.

Keiluweit, M., Nico, P. S., Kleber, M., and Fendorf, S.: Are oxygen limitations under recognized regulators of organic carbon turnover in upland soils?, Biogeochemistry, 127, 157-171, https://doi.org/10.1007/s10533-015-0180-6, 2016.

Keiluweit, M., Gee, K., Denney, A., and Fendorf, S.: Anoxic microsites in upland soils dominantly controlled by clay content, Soil Biol. Biochem., 118, 42-50, https://doi.org/10.1016/j.soilbio.2017.12.002, 2018.

Knowles, R.: Denitrification, Microbiol. Rev., 46, 43-70, 1982.

Kravchenko, A. N., Guber, A. K., Quigley, M. Y., Koestel, J., Gandhi, H., and Ostrom, N. E.: X-ray computed tomography to predict soil N_2O production via bacterial denitrification and N_2O emission in contrasting bioenergy cropping systems, GCB Bioenergy, 10, 894-909, https://doi.org/10.1111/gcbb.12552, 2018.

Kravchenko, A. N., Guber, A. K., Razavi, B. S., Koestel, J., Quigley, M. Y., Robertson, G. P., and Kuzyakov, Y.: Microbial spatial footprint as a driver of soil carbon stabilization, Nature Communications, 10, 3121, https://doi.org/10.1038/s41467-019-11057-4, 2019.

Kremen, A., Bear, J., Shavit, U., and Shaviv, A.: Model demonstrating the potential for coupled nitrification denitrification in soil aggregates, Environmental Science & Technology, 39, 4180-4188, https://doi.org/10.1021/es048304z, 2005.

Kuzyakov, Y.: Microbial hotspots and hot moments in soil: Concept & review, Soil Biol. Biochem., v. 83, pp. 184-199-2015 v.2083, https://doi.org/10.1016/j.soilbio.2015.01.025, 2015.

Legland, D., Arganda-Carreras, I., and Andrey, P.: MorphoLibJ: integrated library and plugins for mathematical morphology with ImageJ, Bioinformatics, 32, 3532-3534, 2016.

Lewicka-Szczebak, D., Well, R., Giesemann, A., Rohe, L., and Wolf, U.: An enhanced technique for automated determination of ^{15}N signatures of N_2, (N_2+N_2O) and N_2O in gas samples, Rapid Commun. Mass Spec., 27, 1548-1558, https://doi.org/10.1002/rcm.6605, 2013.

Lewicka-Szczebak, D., Augustin, J., Giesemann, A., and Well, R.: Quantifying N_2O reduction to N_2 based on N_2O isotopocules – validation with independent methods (helium incubation and ^{15}N gas flux method), Biogeosciences, 14, 711-732, doi: 10.5194/bg-14-711-2017, 2017.

Li, C. S., Frolking, S., and Frolking, T. A.: A model of nitrous oxide evolution from soil driven by rainfall events: 1. Model structure and sensitivity, J. Geophys. Res.-Atmos., 97, 9759-9776, https://doi.org/10.1029/92jd00509, 1992.

Malique, F., Ke, P., Boettcher, J., Dannenmann, M., and Butterbach-Bahl, K.: Plant and soil effects on denitrification potential in agricultural soils, Plant and Soil, 439, 459-474, 10.1007/s11104-019-04038-5, 2019.

Mathieu, O., Lévêque, J., Hénault, C., Milloux, M. J., Bizouard, F., and Andreux, F.: Emissions and spatial variability of N_2O, N_2 and nitrous oxide mole fraction at the field scale, revealed with ^{15}N isotopic techniques, Soil Biol. Biochem., 38, 941-951, https://doi.org/10.1016/j.soilbio.2005.08.010, 2006.

Millington, R., and Quirk, J. P.: Permeability of porous solids, Transactions of the Faraday Society, 57, 1200-&, https://doi.org/10.1039/tf9615701200, 1961.

Millington, R. J., and Quirk, J. M.: Transport in porous media, in: F.A. Van Beren et. al (ed.), Trans. Int. Congr. Soil Sci., 7th, Madison, WI. 14–21 Aug, Elsevier, Amsterdam, 97–106, 1960.

Moldrup, P., Olesen, T., Yamaguchi, T., Schjønning, P., and Rolston, D. E.: Modeling diffusion and reaction in soils: IX. The Buckingham-Burdine-Campbell equation for gas diffusivity in undisturbed soil, Soil Science, 164, 542-551, 1999.

Moldrup, P., Olesen, T., Gamst, J., Schjonning, P., Yamaguchi, T., and Rolston, D. E.: Predicting the gas diffusion coefficient in repacked soil: Water-induced linear reduction model, Soil Sc. Soc. Am. J., 64, 1588-1594, https://doi.org/10.2136/sssaj2000.6451588x, 2000.

Moldrup, P., Olesen, T., Komatsu, T., Schjønning, P., and Rolston, D. E.: Tortuosity, diffusivity, and permeability in the soil liquid and gaseous phases, Soil Sc. Soc. Am. J., 65, 613-623, https://doi.org/10.2136/sssaj2001.653613x, 2001.

Morley, N. J., Richardson, D. J., and Baggs, E. M.: Substrate induced denitrification over or under estimates shifts in soil N_2/N_2O ratios, Plos One, 9, 6, https://doi.org/10.1371/journal.pone.0108144, 2014.

Moyano, F. E., Vasilyeva, N., Bouckaert, L., Cook, F., Craine, J., Curiel Yuste, J., Don, A., Epron, D., Formanek, P., Franzluebbers, A., Ilstedt, U., Kätterer, T., Orchard, V., Reichstein, M., Rey, A., Ruamps, L., Subke, J. A., Thomsen, I. K., and Chenu, C.: The moisture response of soil heterotrophic respiration: interaction with soil properties, Biogeosciences, 9, 1173-1182, https://doi.org/10.5194/bg-9-1173-2012, 2012.

Müller, C., and Clough, T. J.: Advances in understanding nitrogen flows and transformations: gaps and research pathways, J. Agric. Sci., 152, S34-S44, https://doi.org/10.1017/s0021859613000610, 2014.

Nengsih, T. A., Bertrand, F., Maumy-Bertrand, M., and Meyer, N.: Determining the number of components in PLS regression on incomplete data set, Stat. Appl. Genet. Mol. Biol., 18, 28, https://doi.org/10.1515/sagmb-2018-0059, 2019.

Otsu, N.: A threshold selection method from gray-level histograms, Automatica, 11, 23-27, 1975.

Philippot, L., Hallin, S., and Schloter, M.: Ecology of denitrifying prokaryotes in agricultural soil, in: Advances in Agronomy, edited by: Donald, L. S., Academic Press, 249-305, 2007.

Porre, R. J., van Groenigen, J. W., De Deyn, G. B., de Goede, R. G. M., and Lubbers, I. M.: Exploring the relationship between soil mesofauna, soil structure and N_2O emissions, Soil Biol. Biochem., 96, 55-64, https://doi.org/10.1016/j.soilbio.2016.01.018, 2016.

R Core Team: R: A language and environment for statistical computing. R Foundation for Statistical Computing, Vienna, Austria. URL https://www.R-project.org/, 2018.

Rabot, E., Lacoste, M., Henault, C., and Cousin, I.: Using X-ray computed tomography to describe the dynamics of nitrous oxide emissions during soil drying, Vadose Zone J., 14, 10, https://doi.org/10.2136/vzj2014.12.0177, 2015.

Reichstein, M., and Beer, C.: Soil respiration across scales: The importance of a model-data integration framework for data interpretation, Journal of Plant Nutrition and Soil Science, 171, 344-354, https://doi.org/10.1002/jpln.200700075, 2008.

Resurreccion, A. C., Moldrup, P., Kawamoto, K., Hamamoto, S., Rolston, D. E., and Komatsu, T.: Hierarchical, bimodal model for gas diffusivity in aggregated, unsaturated soils, Soil Sc. Soc. Am. J., 74, 481-491, https://doi.org/10.2136/sssaj2009.0055, 2010.

Ryan, M. G., and Law, B. E.: Interpreting, measuring, and modeling soil respiration, Biogeochemistry, 73, 3-27, https://doi.org/10.1007/s10533-004-5167-7, 2005.

Scheer, C., Fuchs, K., Pelster, D. E., and Butterbach-Bahl, K.: Estimating global terrestrial denitrification from measured N_2O:(N_2O+N_2) product ratios, Current Opinion in Environmental Sustainability, 47, 72-80, https://doi.org/10.1016/j.cosust.2020.07.005, 2020.

Schindelin, J., Arganda-Carreras, I., Frise, E., Kaynig, V., Longair, M., Pietzsch, T., Preibisch, S., Rueden, C., Saalfeld, S., and Schmid, B.: Fiji: an open-source platform for biological-image analysis, Nature methods, 9, 676-682, 2012.

Schlüter, S., Sheppard, A., Brown, K., and Wildenschild, D.: Image processing of multiphase images obtained via X-ray microtomography: A review, Water Resources Research, 50, 3615-3639, https://doi.org/10.1002/2014wr015256, 2014.

Schlüter, S., Leuther, F., Vogler, S., and Vogel, H.-J.: X-ray microtomography analysis of soil structure deformation caused by centrifugation, Solid Earth, 7, 129-140, 2016.

Schlüter, S., Zawallich, J., Vogel, H. J., and Dorsch, P.: Physical constraints for respiration in microbial hotspots in soil and their importance for denitrification, Biogeosciences, 16, 3665-3678, https://doi.org/10.5194/bg-16-3665-2019, 2019.

Senbayram, M., Chen, R., Budai, A., Bakken, L., and Dittert, K.: N_2O emission and the $N_2O/(N_2O+N_2)$ product ratio of denitrification as controlled by available carbon substrates and nitrate concentrations, Agriculture, Ecosystems & Environment, 147, 4-12, https://doi.org/10.1016/j.agee.2011.06.022, 2012.

Sexstone, A. J., Revsbech, N. P., Parkin, T. B., and Tiedje, J. M.: Direct measurement of oxygen profiles and denitrification rates in soil aggregates, Soil Sc. Soc. Am. J., 49, 645-651, 1985.

Shoun, H., Kim, D.-H., Uchiyama, H., and Sugiyama, J.: Denitrification by fungi, FEMS Microbiol. Lett., 94, 277-281, 1992.

Smith, K. A., Ball, T., Conen, F., Dobbie, K. E., Massheder, J., and Rey, A.: Exchange of greenhouse gases between soil and atmosphere: interactions of soil physical factors and biological processes, European Journal of Soil Science, 54, 779-791, https://doi.org/10.1046/j.1351-0754.2003.0567.x, 2003.

Spott, O., Russow, R., Apelt, B., and Stange, C. F.: A ^{15}N-aided artificial atmosphere gas flow technique for online determination of soil N_2 release using the zeolite Köstrolith SX6®, Rapid Commun. Mass Spec., 20, 3267-3274, https://doi.org/10.1002/rcm.2722, 2006.

Surey, R., Lippold, E., Heilek, S., Sauheitl, L., Henjes, S., Horn, M. A., Mueller, C. W., Merbach, I., Kaiser, K., Böttcher, J., and Mikutta, R.: Differences in labile soil organic matter explain potential denitrification and denitrifying communities in a long-term fertilization experiment, Appl. Soil. Ecol., 153, 103630, https://doi.org/10.1016/j.apsoil.2020.103630, 2020.

Syakila, A., and Kroeze, C.: The global nitrous oxide budget revisited, Greenhouse Gas Measurement and Management, 1, 17-26, https://doi.org/10.3763/ghgmm.2010.0007, 2011.

Thompson, R. L., Lassaletta, L., Patra, P. K., Wilson, C., Wells, K. C., Gressent, A., Koffi, E. N., Chipperfield, M. P., Winiwarter, W., Davidson, E. A., Tian, H., and Canadell, J. G.: Acceleration of global N_2O emissions seen from two decades of atmospheric inversion, Nature Climate Change, 9, 993-998, https://doi.org/10.1038/s41558-019-0613-7, 2019.

Tian, H., Xu, R., Canadell, J. G., Thompson, R. L., Winiwarter, W., Suntharalingam, P., Davidson, E. A., Ciais, P., Jackson, R. B., Janssens-Maenhout, G., Prather, M. J., Regnier, P., Pan, N., Pan, S., Peters, G. P., Shi, H., Tubiello, F. N., Zaehle, S., Zhou, F., Arneth, A., Battaglia, G., Berthet, S., Bopp, L., Bouwman, A. F., Buitenhuis, E. T., Chang, J., Chipperfield, M. P., Dangal, S. R. S., Dlugokencky, E., Elkins, J. W., Eyre, B. D., Fu, B., Hall, B., Ito, A., Joos, F., Krummel, P. B., Landolfi, A., Laruelle, G. G., Lauerwald, R., Li, W., Lienert, S., Maavara, T., MacLeod, M., Millet, D. B., Olin, S., Patra, P. K., Prinn, R. G., Raymond, P. A., Ruiz, D. J., van der Werf, G. R., Vuichard, N., Wang, J., Weiss, R. F., Wells, K. C., Wilson, C., Yang, J., and Yao, Y.: A comprehensive quantification of global nitrous oxide sources and sinks, Nature, 586, 248-256, 10.1038/s41586-020-2780-0, 2020.

Tiedje, J. M.: Ecology of denitrification and dissimilatory nitrate reduction to ammonium, in: Environmental Microbiology of Anaerobes, edited by: Zehnder, A. J. B., John Wiley and Sons, N.Y., 179-244, 1988.

Ussiri, D., and Lal, R.: Soil emission of nitrous oxide and its mitigation, Springer, 2013.

van Cleemput, O.: Subsoils: chemo- and biological denitrification, N_2O and N_2 emissions, Nutrient Cycling in Agroecosystems, 52, 187-194, https://doi.org/10.1023/a:1009728125678, 1998.

Wickham, H.: ggplot2: Elegant Graphics for Data Analysis. Springer-Verlag New York, 2016.

Wiegmann, A., and Bube, K. P.: The explicit-jump immersed interface method: Finite difference methods for PDEs with piecewise smooth solutions, SIAM J. Numer. Anal., 37, 827-862, https://doi.org/10.1137/S0036142997328664, 2000.

Wiegmann, A., and Zemitis, A.: EJ-HEAT: A fast explicit jump harmonic averaging solver for the effective heat conductivity of composite materials, Berichte des Fraunhofer ITWM, 94, 2006.

Wolodzko, T.: Kernelboot: Smoothed bootstrap and random generation from kernel densities, 2020.

Zumft, W. G.: Cell biology and molecular basis of denitrification, Microbiology and Molecular Biology Reviews, 61, 533-616, 1997.

Supplementary Material for Denitrification in soil as a function of oxygen supply and demand at the microscale

Lena Rohe[1], Bernd Apelt[1], Hans-Jörg Vogel[1], Reinhard Well[2], Gi-Mick Wu[3], Steffen Schlüter[1]

[1]Helmholtz Centre for Environmental Research – UFZ, Department Soil System Sciences, Theodor-Lieser-~~5~~ Str. 4, 06120 Halle, Germany

[2]Thünen Institute of Climate Smart Agriculture, Bundesallee 65, 38116 Braunschweig, Germany

[3]Helmholtz Centre for Environmental Research – UFZ, PACE, Permoserstraße 15, 04318 Leipzig, Germany

Correspondence to: Lena Rohe, (lena.rohe@ufz.de)

Detailed information on pre-incubation, determination of water holding capacity and experimental set-up (Section 2: Material and Methods, 1. Incubation)

For pre-incubation the soil was loosely placed on a tray, adjusted to 50% water holding capacity (WHC) with a spray can and stored at room temperature in the dark for two weeks.

Additional soil cores with the same dimension were packed in an identical manner as described in the Material and Method section and fully saturated by immersion in a water bath for 24h. The water-holding capacity (v/v % WHC) for each soil material was determined after free drainage. These water volumes were taken as a reference to adjust the above-mentioned saturation levels (70, 83 and 95% WHC). Note that WHC values are not identical to water saturations expressed in v/v% water-filled pore space (WFPS), since 100%WHC covers a smaller volume than the total pore volume due to 1) air entrapment during full immersion in water and 2) drainage of the biggest pores in a pressure head range of -10 to 0 cm in a 10 cm tall, freely draining sample.

The cylindrical PVC columns containing the packed soil aggregates (698.41 cm^3) were closed tightly by sealing caps at the top and bottom. The closed column was equipped with an in- and outlet to allow flushing the headspace (69.83 cm^3) through steel capillaries (total volume 1.33 cm^3). A maximal evaporation loss during incubation of one soil core is estimated to be around 1.22 g H_2O. A temperature sensor (PT100) was installed through the centre of the lid reaching the repacked aggregates with a depth of ca 3 cm down to assure constant temperature of 20°C during incubation.

Table with average data for each treatment (WFPS and aggregate size) with average values of CO_2, N_2O and (N_2O+N_2) fluxes, O_2 saturation, total porosity, visible air content (ε_{vis}), connected air content (ε_{con}), anaerobic soil volume fraction (ansvf), simulated diffusivity (D_{sim}) and product ratio (pr) for soil from Gießen (GI) and Rotthalmünster (RM)

Table S1: Average values for CO_2, N_2O and (N_2O+N_2) fluxes, O_2 saturation, visible air content (ε_{vis}), connected air content (ε_{con}), anaerobic soil volume fraction (*ansvf*), simulated diffusivity (D_{sim}) and product ratio (*pr*) [$N_2O/(N_2O+N_2)$]. Standard error (n=3) is shown in the brackets.

soil	WFPS [%]	Aggregate size [mm]	CO_2-C [µg h^{-1} kg^{-1}]	N_2O-N [µg h^{-1} kg^{-1}]	(N_2O+N_2)-N [µg h^{-1} kg^{-1}]	O_2 [%air saturation]	Total porosity [-]	ε_{vis} [-]	ε_{con} [-]	*ansvf* [-]	D_{sim} [m^2 s^{-1}]	*pr* [-]
GI	63	2-4	535.71 (72.95)	0.26 (0.07)	2.94 (1.75)	47.99 (1.30)	0.21 (0.03)	0.21 (0.03)	0.20 (0.03)	<0.01 (<0.01)	$1.09\ 10^{-06}$ ($1.82\ 10^{-08}$)	0.34 (0.16)
GI	63	4-8	503.19 (65.9)	1.28 (0.67)	2.93 (0.45)	55.69 (1.87)	0.20 (0.02)	0.20 (0.02)	0.20 (0.02)	<0.01 (<0.01)	$1.08\ 10^{-06}$ ($1.56\ 10^{-08}$)	0.44 (0.09)
GI	75	2-4	617.30 (53.06)	18.01 (3.00)	35.53 (2.15)	56.48 (2.50)	0.18 (0.03)	0.13 (0.03)	0.12 (0.03)	0.04 (0.02)	$1.59\ 10^{-08}$ ($7.26\ 10^{-09}$)	0.52 (0.08)
GI	75	4-8	548.66 (57.25)	17.89 (1.94)	26.90 (4.42)	61.78 (2.22)	0.19 (0.03)	0.14 (0.03)	0.11 (0.04)	0.21 (0.07)	$2.76\ 10^{-09}$ ($2.32\ 10^{-09}$)	0.68 (0.06)
GI	85	2-4	175.33 (71.30)	18.74 (7.51)	27.20 (6.41)	33.77 (1.47)	0.18 (0.03)	0.12 (0.02)	0.03 (0.03)	0.79 (0.14)	$5.59\ 10^{-10}$ ($3.36\ 10^{-10}$)	0.64 (0.09)
GI	85	4-8	125.62 (21.69)	13.30 (4.45)	21.38 (1.97)	39.89 (2.55)	0.20 (0.03)	0.10 (0.02)	0.01 (0.02)	0.80 (0.09)	$2.00\ 10^{-10}$ ($4.00\ 10^{-11}$)	0.60 (0.10)
RM	65	2-4	144.85 (20.45)	0.02 (0.01)	NA	55.11 (2.20)	0.16 (0.03)	0.16 (0.03)	0.15 (0.03)	<0.01 (<0.01)	$2.24\ 10^{-07}$ ($1.39\ 10^{-08}$)	n.d.
RM	65	4-8	158.06 (21.05)	0.05 (0.03)	0.66 (0.54)	48.95 (2.56)	0.15 (0.03)	0.15 (0.03)	0.15 (0.03)	<0.01 (<0.01)	$2.08\ 10^{-07}$ ($2.69\ 10^{-08}$)	0.08 (0.04)
RM	78	2-4	174.29 (4.14)	4.28 (2.04)	6.86 (3.28)	59.16 (2.88)	0.14 (0.03)	0.10 (0.03)	0.09 (0.03)	0.08 (0.06)	$1.03\ 10^{-08}$ ($3.65\ 10^{-09}$)	0.65 (0.08)
RM	78	4-8	142.69 (26.87)	6.00 (1.18)	9.88 (1.91)	53.41 (2.60)	0.14 (0.03)	0.10 (0.03)	0.07 (0.04)	0.34 (0.22)	$1.47\ 10^{-08}$ ($7.34\ 10^{-09}$)	0.61 (0.05)
RM	88	2-4	50.60 (7.49)	5.07 (0.96)	8.46 (2.48)	22.61 (1.95)	0.10 (0.02)	0.06 (0.02)	0.03 (0.02)	0.69 (0.10)	$3.27\ 10^{-11}$ ($2.02\ 10^{-11}$)	0.64 (0.06)
RM	88	4-8	46.89 (10.41)	5.60 (1.15)	8.50 (1.92)	42.01 (2.59)	0.13 (0.03)	0.07 (0.02)	0.02 (0.01)	0.74 (0.07)	$2.03\ 10^{-09}$ ($1.76\ 10^{-09}$)	0.67 (0.04)

n.d.: not detectable; NA: not applicable

N_2O and CO_2 fluxes and O_2 saturation as a function of incubation time

N_2O and CO_2 fluxes (Figure S1) and O_2 saturation at 7 locations within the soil core (Figure S2) were measured during the incubation time of approximately 192h. In the beginning of incubation establishment of equilibrium was assumed and therefore 24h of measurements in the beginning of the incubation time were excluded.

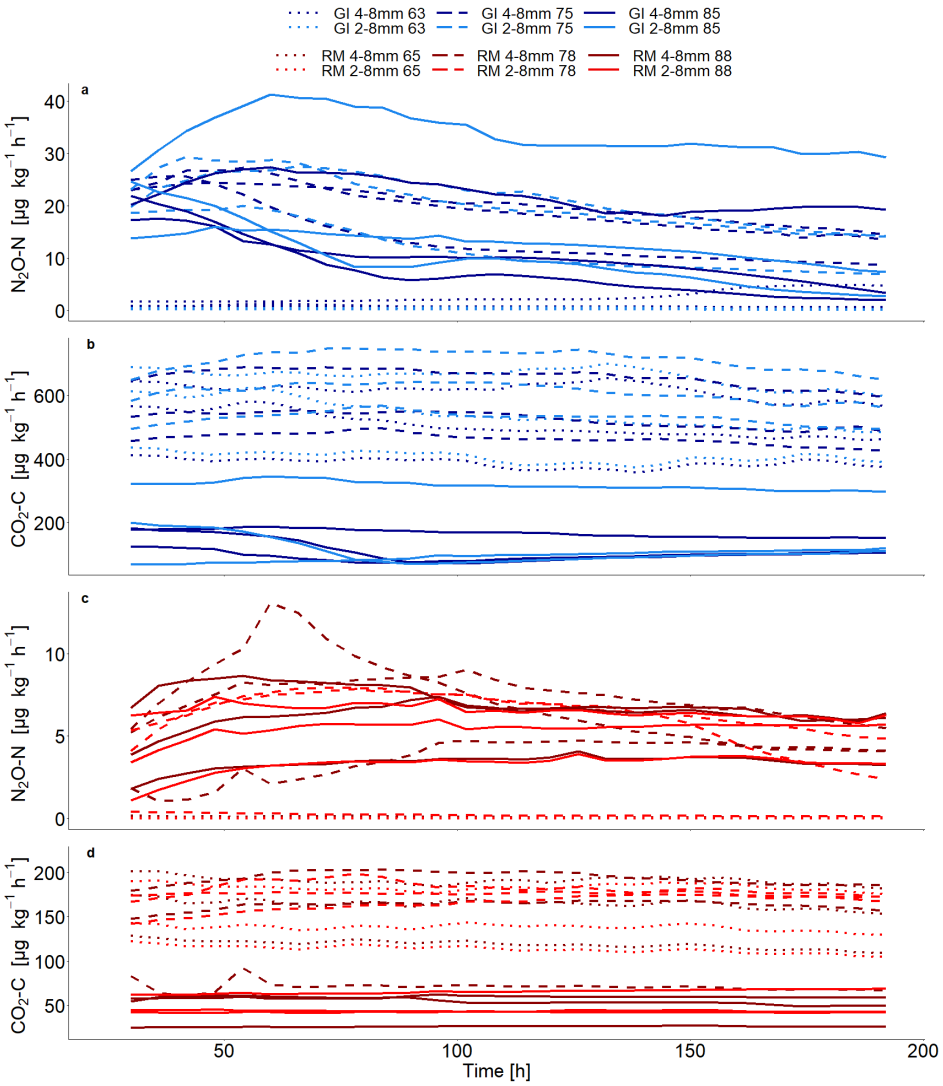

Figure S1: Average N_2O and CO_2 fluxes as a function of incubation time for soil from Rotthalmünster (RM) in red and Gießen (GI) in blue, two aggregate sizes (2-4 and 4-8 mm) and three water saturations (dotted, dashed or solid line depicted lowest, medium and highest water saturation, respectively) with three replicates.

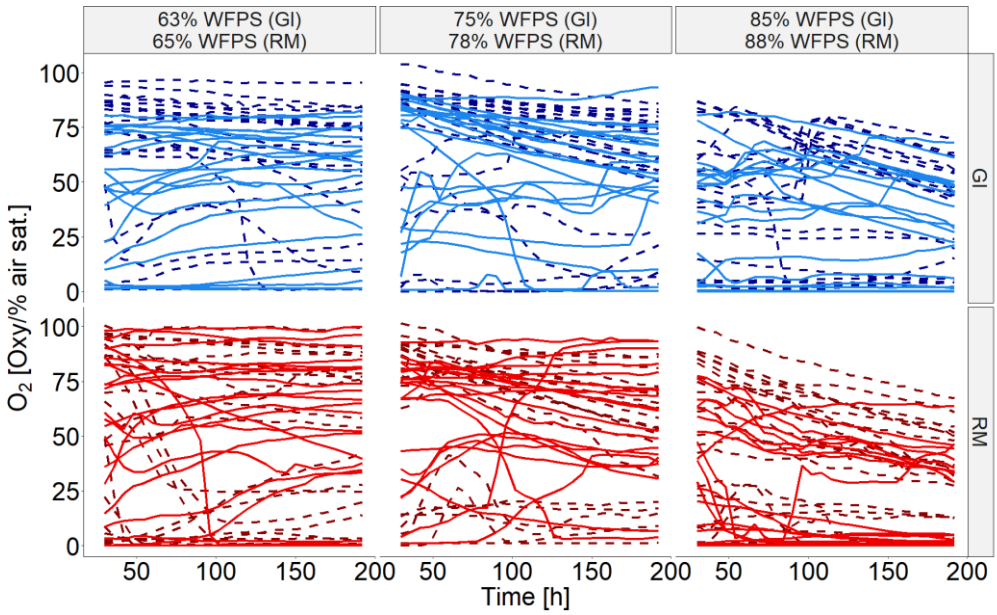

Figure S2: Average O_2 saturations measured by 7 sensors per soil core as a function of incubation time for soil from Rotthalmünster (RM) in red and Gießen (GI) in blue, two aggregate sizes (2-4 and 4-8 mm (solid and dashed lines, respectively)) and three water saturations with three replicates each.

Detailed description of calculating different pools for ^{15}N

The fraction of N in N_2O ($f_p\_N_2O$) or N_2 ($f_p\_N_2$) originating from ^{15}N-labelled NO_3^- pool within one sample was calculated according to (Spott et al., 2006; Lewicka-Szczebak et al., 2013; Well et al., 2019) using the ^{15}N abundance of N_2 or N_2O measured in the analyzed gas sample (a_m), in the non-labelled N_2 in technical gas (a_{bgd}), and the calculated ^{15}N abundance of the active NO_3^- pool (a_p).

$$f_p\_N_2O = \frac{a_m - a_{bgd}}{a_p - a_{bgd}} \quad (1)$$

$$f_p\_N_2 = \frac{a_m - a_{bgd}}{a_p - a_{bgd}} \quad (2)$$

with

$$a_m = \frac{^{29}R + 2\,^{30}R}{2(1 + ^{29}R + ^{30}R)} \quad (3)$$

and using the fraction of $^{30}N_2$ in the gas sample ($^{30}\chi_m$):

$$a_p = \frac{^{30}\chi_m - a_m \cdot a_{bgd}}{a_m - a_{bgd}} \quad (4)$$

This is based on the a non-random distribution of isotopes in N_2O and N_2 (Spott et al., 2006):

$$^{30}\chi_m = \frac{^{30}R}{1 + ^{29}R + ^{30}R} \quad (5)$$

Thus, with $f_p\_N_2O$ the N_2O flux from denitrification (N_2O_deni) was calculated

$$N_2O\_deni = N_2O\_total * f_p\_N_2O \quad (6)$$

The $f_p\_N_2O$ was constantly near 1 for both soils, aggregate sizes, water saturations and time points of sampling resulting in very similar N_2O_total and N_2O_deni values (Figure S3). The time resolution for N_2O_total was much higher than for isotopic analysis and therefore N_2O_total was used to calculate N_2O fluxes from denitrification and for statistical analysis.

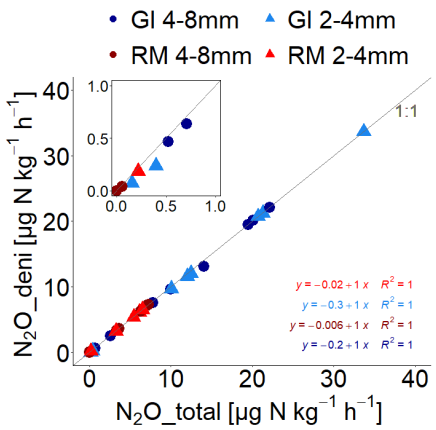

Figure S3: Comparison of total N_2O emissions (N_2O_total) captured by gas chromatography and N_2O emissions from denitrification (N_2O_deni) from experimental treatments with soil from Rotthalmünster (RM) and Gießen (GI), two aggregate sizes (2-4 and 4-8 mm) and three water saturations. Goodness of fit to the 1:1 line (gray line) is expressed as slope and R^2 from linear regression.

Impact of packing procedure on visible air content (ε_{vis}) and anaerobic soil volume fraction (ansvf)

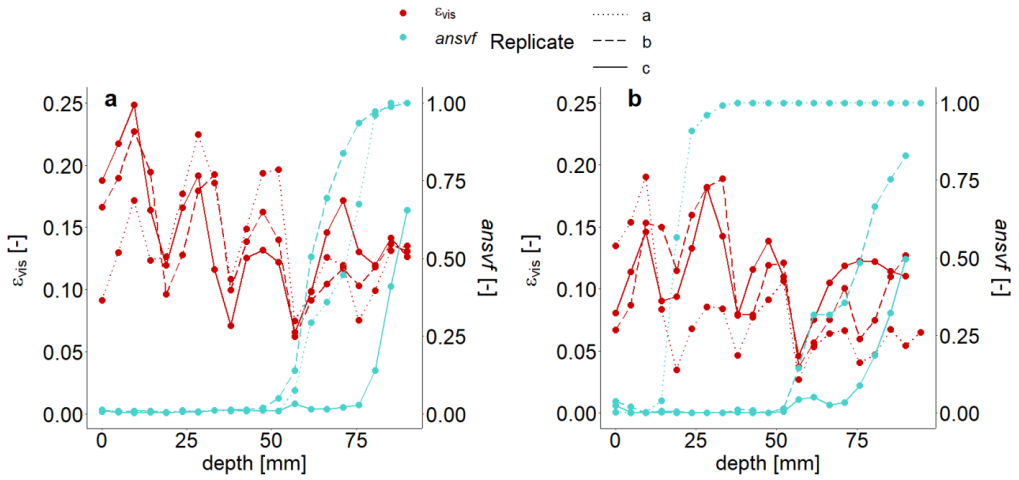

Figure S4: Visible air content (ε_{vis}) and the anaerobic soil volume fraction (*ansvf*) as a function of soil core depth for soil from (a) Gießen (GI) and (b) Rotthalmünster (RM). Shown here are examples of 3 replicates of repacked soil cores with aggregates of 4-8 mm size incubated at medium water saturation of 75% with GI and 78% with RM soil. Values shown here for air content and anaerobic soil volume fraction are aggregated for 4.7 mm segments in depth.

Two representative examples of one treatment were chosen to illustrate the impact of packing the soil on visible air content (ε_{vis}) and anaerobic soil volume fraction (*ansvf*) (large aggregates of GI soil incubated at 75% WFPS and large aggregates of RM soil incubated at 78 % WFPS) (Figure S4). During the packing procedure, intervals of 2 cm were the best option to adjust the target material-specific bulk densities and water saturations within the soil core. The average ε_{vis} did not differ between replicates of one treatment (Figure 4), but decreased with increasing depth of the packed soil core and was extremely reduced at the top of one packing interval (Figure S4). This varying compaction in different layers affected also the *ansvf* of each repacked core (Figure S4). The *ansvf* dramatically increased in layers, where lowest ε_{vis} was observed. In some cases, the *ansvf* even reached 1, i.e. complete exclusion from connected air-filled pores.

Detailed information on simulated diffusivity (D_{sim})

Diffusivity was simulated for individual aggregates as well as for the entire soil core (bulk diffusivity) directly on segmented X-ray CT data on a workstation with Intel® Xeon® CPUs (E7-8867v4, 2.46Hz, 36 cores) and 6.1TB RAM by solving the Laplace equation with the DiffuDict module in the GeoDict 2019

Software (Math2Market GmbH, Kaiserslautern, Germany). A hierarchical approach was used to estimate the effective diffusivity of the wet soil matrix by simulating Laplace diffusion on cubes contained in individual soil aggregates with the Explicit Jump solver assuming free diffusion in the visible pore space, a completely impermeable background and symmetric boundary condition on all sides (Wiegmann and Zemitis, 2006; Wiegmann and Bube, 2000). The resulting effective diffusion coefficient is expressed as a percentage of the diffusion coefficient in the free fluid and was in the range of $6.6\ 10^{-4} \pm 3.7\ 10^{-4}$% and $2.4\ 10^{-2} \pm 1.3\ 10^{-2}$% for wet aggregates of RM and GI soil, respectively. For the soil cores with <70% WFPS the visible pore space in the high-resolution aggregate images is assumed to be air-filled, whereas for soil cores with ≥75% WFPS it is assumed to be water-filled, which is justified by the fact that 1) the air-filled porosity at <70% WFPS in individual aggregates (RM: 17.6%, GI: 23.1%) exceeds the visible pore space in low-resolution soil core images (RM: 15.8%, GI: 20.6%) and 2) that in contrast to the higher moisture levels no free water could be identified at the column scale with air-filled porosity at <70% WFPS. Thus, the effective diffusion coefficient for soil matrix is determined with respect to the oxygen diffusion coefficient (D_{O2}) at 2% O_2 in pure air ($2.03\ 10^{-5}$ m² s^{-1}) and in pure water ($1.97\ 10^{-9}$ m² s^{-1}) at 20°C, respectively (http://compost.css.cornell.edu/oxygen/oxygen.diff.air.html).

Another series of diffusion experiments was modeled with the Explicit Jump solver on the entire soil cores (1550x1550x [1500-1600] voxels) with the effective diffusion coefficient of the soil matrix taken from aggregate simulations, an impermeable exterior, impermeable mineral grains (GI only) and the diffusion coefficient of oxygen in air and water (≥70% WFPS only) in the respective material classes. In order to save memory, periodic boundary conditions were assumed on all sides. This is irrelevant for lateral boundaries as they are blocked by the impermeable exterior anyway, but may lead to a lower effective diffusion coefficient, since the spatial distribution of materials at the top and bottom of the domain do not match, which imposes an additional diffusion barrier. The reduction by this discontinuity was in the range of $5.1\ 10^{-9}$ to $6.7\ 10^{-8}$ $m^2\ s^{-1}$ in small test images (500^3 voxels) from all soil materials and saturations.

Product ratio (pr) as a function of time

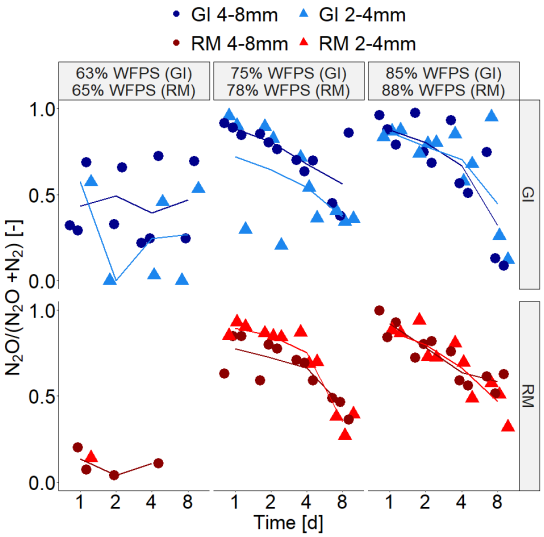

Figure S5: Product ratio (*pr*) [$N_2O/(N_2O+N_2)$] as a function of time for soil from Gießen (GI) in blue and Rotthalmünster (RM) in red with aggregates of 2-4 mm and 4-8mm size incubated at three water saturations. The lines connect the average values of three replicates (large and small aggregates, respectively).

Correlation between ansvf and gas emissions and concentrations ~~and emissions~~

The correlation of *ansvf* with average gas fluxes and internal O_2 concentrations is shown in Figure ~~5~~S6. Since the drop in CO_2 release at the highest water saturations coincided with an escalating *ansvf*, the relation between the two was highly correlated (Spearman's R>-0.7 and p=0.04) for all soils and aggregate sizes (Figure ~~5~~S6a), but with different slopes for both soils due to vastly different SOM contents. The correlation of *ansvf* with N_2O is weaker (Spearman's $0.6<R<0.77$) and on the verge of being significant ($p\leq0.1$) (Figure ~~5~~S6c). However, the correlation of *ansvf* with (N_2O+N_2) release is even worse (p>0.2), so the mechanisms that govern N_2O and (N_2O+N_2) release must be more complex (Figure ~~5~~S6c, d). As expected the average O_2 saturation decreases with increasing *ansvf* (Figure ~~5~~S6b). Yet, correlation is lower than for CO_2 (Spearman's $-0.6<R<-0.2$, but p>0.2), likely due to limited representativeness of average O_2 concentrations derived from a few point measurements.

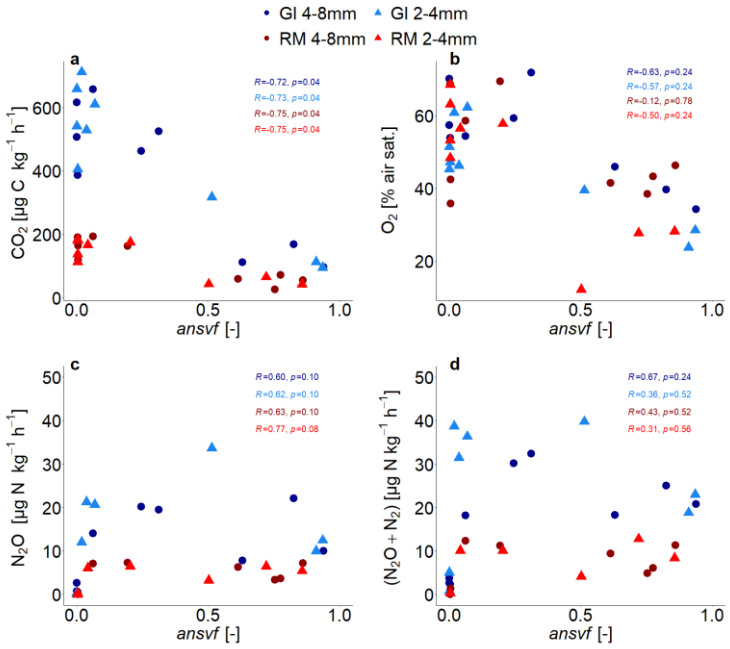

Figure S6: Average (a) CO_2, fluxes (b) O_2 saturation, (c) N_2O and (d) (N_2O+N_2) fluxes as a function of anaerobic soil volume fraction (*ansvf*) for soil from Rotthalmünster (RM) and Gießen (GI) and two aggregate sizes (2-4 and 4-8 mm) for three individual replicates. The Spearman's rank correlation coefficient (*R*) result from Spearman's rank correlation and indicate the extent of monotonic relation between the ranks of both variables. The associated p-values (*p*) were corrected for multiple comparison according to Benjamini and Hochberg (1995).

Correlation matrix between all ~~predictors~~variables

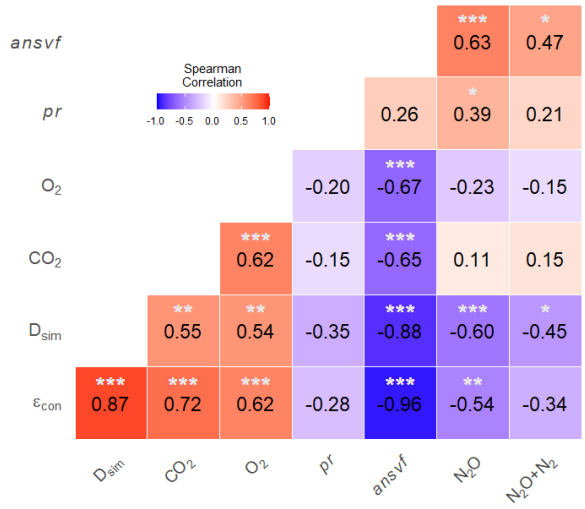

Figure ~~S6~~S7: Correlation matrix of Spearman's rank correlation showing coefficients (*R*) between two measured variables (N_2O, (N_2O+N_2) or CO_2 fluxes, anaerobic soil volume fraction (*ansvf*), product ratio (*pr*), O_2 saturation (O_2), simulated diffusivity (D_{sim}) or connected air content (ε_{con})) in one cell with pairwise deletion of missing values. Asterisks indicate the statistical significance with significance levels of *p ≤ 0.05, **p ≤ 0.005, ***p ≤ 0.001 for adjusted p-values according to the method of Benjamini and Hochberg (1995). Color scheme indicate low (light colors) or strong (intensive colors) correlation as well as positive (red) or negative (blue) correlation.

Explanatory variables for denitrification

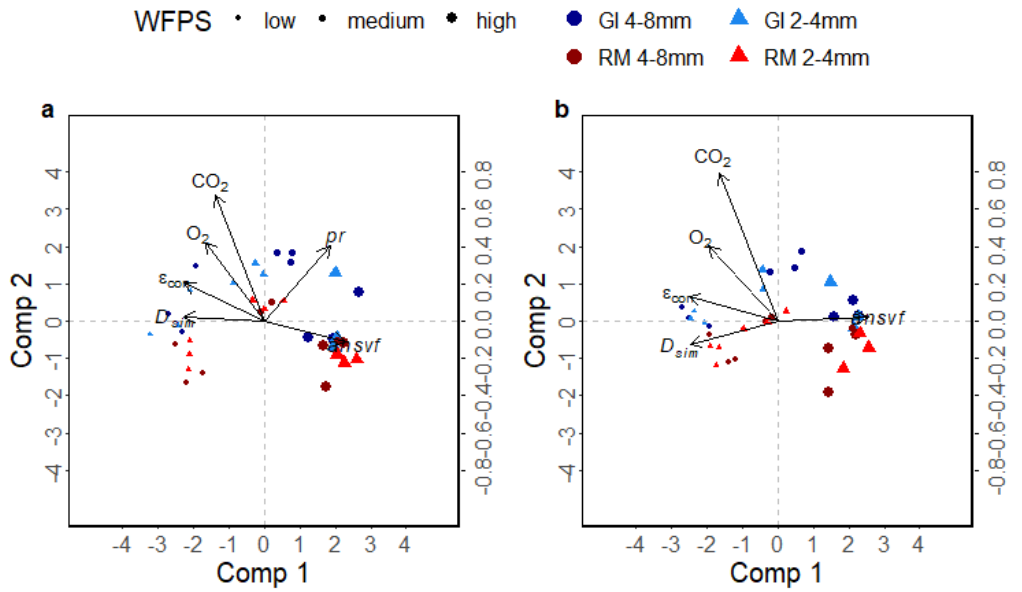

Figure ~~S7~~S8: Biplot of the PLSR results for response variables N_2O (a) and (N_2O+N_2) fluxes (b) showing x-scores and x-loadings of two components (Comp 1 and Comp 2). The x- and y- axis represent values of the scores for soil from Gießen (GI) in blue and Rotthalmünster (RM) in red with aggregates of 2-4 mm (triangles) and 4-8 mm size (circles) incubated at three water saturations depicted by the size of symbols. The second y-axis represents values for the loadings (predictors and arrows) to show the influence of variables on the components.

The regression equations with R^2 values and a confidence interval of 95% in square brackets resulting from PLSR with CO_2, (*pr*) and *ansvf* as explanatory variables to predict N_2O or (N_2O+N_2) fluxes of the present study for data after log- or logit transformation:

$$\log(N_2O) = 0.54\log(CO_2) + 0.35\ \text{logit}(ansvf) + 0.55\ pr - 0.32\log(D_{sim}) - 0.18\ \varepsilon_{con} + 0.11\ O_2; \quad (7)$$

R^2 = 0.82 [0.65-0.91]

$$\log(N_2O + N_2) = 0.95\log(CO_2) + 0.60\ \text{logit}(ansvf) - 0.56\log(D_{sim}) - 0.31\ \varepsilon_{con} + 0.10\ O_2\ ; \quad (8)$$

R^2 = 0.78 [0.62-0.85]

~~The regression equations with R^2 values and a confidence interval of 95% in square brackets resulting from PLSR with CO_2, *ansvf* (and *pr*) identified as most important explanatory variables to predict N_2O or (N_2O+N_2) fluxes of the present study for data after log- or logit transformation:~~

~~$\log(N_2O) = 0.18\log(CO_2) + 0.14\ \text{logit}(ansvf) + 0.15\ pr$; R^2 = 0.71 [0.55-0.83] (9)~~

~~$\log(N_2O + N_2) = 0.35\log(CO_2) + 0.42\ \text{logit}(ansvf)$; R^2 = 0.83 [0.71-0.90] (10)~~

Empirical models to calculate the diffusivity of the soil cores

It is assumed, that the total porosity ([Φ]) was unaffected by the packing procedure, whereas the air content (ε) is expected to differ from the theoretic value due to compact regions and intervals caused by the packing (Figure S4). Following from this, the target bulk density of the repacked soil cores was used to calculate Φ (0.62 or 0.51 for GI and RM soil, respectively), while CT-derived ε was used. This enabled to calculate diffusivity based on the frequently used model of Millington and Quirk (1960), Millington and Quirk (1961), Moldrup et al. (2000) and also according to the model of Deepagoda et al. (2011) (Table S2, Figure S6S9). As expected, diffusivity from these models has a lower explanatory power for N_2O and (N_2O+N_2) release compared to D_{sim} of the present study (3D simulation) (Table S2). Higher diffusivities for treatments ≥75% WFPS from empirical models (D_{emp}) compared to D_{sim} result from heterogeneities in compaction of the repacked soil core as described earlier (Figure S8, Figure S4, Figure S9), while empirical models were developed for natural soils that very likely possess higher air continuity at low air content. These empirical models only take averages for porosity and water-filled pores into account (Millington and Quirk, 1961; Moldrup et al., 2000) (Figure S8S9, Table S2), whereas heterogeneities in compaction are explicitly considered in 3D diffusivity simulations (D_{sim}).

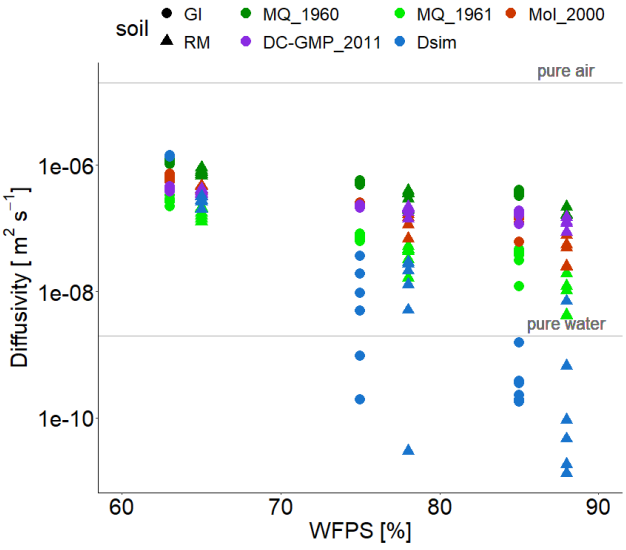

Figure S8S9: Simulated diffusivities (D_{sim}) of the present study and calculated diffusivities as a function of WFPS for both soils (RM and GI). Models used to calculate diffusivity are published by Millington and Quirk (1960) (MQ_1960), Millington and Quirk (1961) (MQ_1961), Moldrup et al. (2000) (Mol_2000) and Deepagoda et al. (2011) (DC_GMP_2011). According to the calculations of the present study diffusivity in free air (D_0) was assumed to be 2.03 10^{-5} m^2 s^{-1}.

Table S2: Explained variability (expressed as R^2) with confidence interval of 95% in square brackets for N_2O and (N_2O+N_2) release obtained from partial least square regression (PLSR) using explanatory variables CO_2, diffusivity (and product ratio (*pr*) for N_2O as response variable only). This was done to assess possibilities to substitute one of the most important explanatory variables (*ansvf*) by diffusivity. Data were pooled for both soils (RM and GI), WFPS treatments and aggregate sizes (n= 36). Diffusivity was obtained by 3D simulation of the present study (D_{sim}) or existing soil gas diffusivity models were used to calculate diffusivity, using total porosity (Φ) and air content (ε) while diffusivity in free air (D_0) is assumed to be 2.03 10^{-5} m^2 s^{-1}.

method	Equation to calculate diffusivity D_{emp} [m^2 s^{-1}]	R^2 with response variable N_2O	R^2 with response variable (N_2O+N_2)
Present study[1]	D_{sim}	0.59 [0.34-0.78]	0.63 [0.39-0.78]
Millington & Quirk (1961) [1]	$(\varepsilon^{10/3}/\Phi^2)$ D_0	0.46 [0.20-0.69]	0.57 [0.28-0.78]
Millington & Quirk (1960) [1]	$(\varepsilon^2/\Phi^{2/3})$ D_0	0.48 [0.22-0.70]	0.52 [0.21-0.74]
Moldrup et al. (2000)[1]	$\varepsilon^{1.5}$ (ε/Φ) D_0	0.59 [0.29-0.79]	0.54 [0.24-0.75]
Deepagoda et al (2011)[1]	$0.1[2(\varepsilon/\Phi)^3+0.04(\varepsilon/\Phi)]$ D_0	0.52 [0.27-0.73]	0.69 [0.42-0.82]
theoretic air content[2]	ε_t	0.55 [0.30-0.76]	0.78 [0.57-0.90]
no diffusivity[3]	-	0.48 [0.16-0.71]	0.07

[1]PLSR with CO_2 and diffusivity (and product ratio (*pr*)) as explanatory variables and N_2O or (N_2O+N_2) as response variables.

[2]Diffusivity substituted by the theoretic air content (ε_t) targeted during packing in PLSR.

[3]Diffusivity was excluded in PLSR resulting in CO_2 (and product ratio (*pr*)) as explanatory variable for N_2O and for (N_2O+N_2). Because CO_2 was the single explanatory variable for (N_2O+N_2) a simple linear model was used to estimate R^2.

Calculation of anaerobic soil volume fraction (ansvf) by (N_2O+N_2) fluxes from oxic and anoxic incubations

To calculate an anaerobic soil volume fraction within the soil cores ($ansvf_{cal}$) independently from the X-ray CT imaging derived *ansvf*, parallel oxic and anoxic incubations were conducted~~-~~ using a different suite of larger repacked soil cores. The conditions for incubations were very similar in soil cores as described before (in the Methods section and Supplementary Material) for oxic incubation. Deviations from the experimental protocol were the dimension of the soil core (10x14.4 cm), unspecific sieving (>10 mm), a flow rate of 20 mL/min and a target saturation of 75% WFPS for both soils (GI and RM). Soil material for all incubations was obtained from the same batches~~, that had been used for the oxic incubations.~~ Batches consisted of approx. 2000kg sieved, homogenized and air-dried soil stored at 6°C that had been collected and prepared to allow the study of comparable soil samples in various labs during several years. After ~~one week with~~three weeks with oxic incubation using a technical gas (20% O_2 and 2% N_2 in pure He) the atmospheric conditions were switched to anoxic conditions (2% N_2 in pure He). N_2O and N_2 fluxes were quantified using the ^{15}N labelling approach as described before. A comparison of oxic and anoxic (N_2O+N_2) fluxes under these comparable conditions is possible because $ansvf_{cal}$ assumes that actual denitrification is linearly related to *ansvf* and that the specific anoxic denitrification rate is homogenous, i.e. would be identical at any location within the soil.

The calculated *ansvf* ($ansvf_{cal}$) derived from incubation (N_2O+N_2) fluxes with oxic ($(N_2O+N_2)_{oxic}$) and anoxic ($(N_2O+N_2)_{anoxic}$) conditions is thus (Table S3):

$$ansvf_{cal} = \frac{(N_2O+N_2)_{oxic}}{(N_2O+N_2)_{anoxic}} \quad (\text{~~11~~}9)$$

Table S3: Average (N_2O+N_2) fluxes with oxic conditions ($(N_2O+N_2)_{oxic}$), ~~present study; n=3)~~ and with anoxic conditions ($(N_2O+N_2)_{anoxic}$), ~~parallel incubations,~~ (n=4) from parallel incubations for soils from Rotthalmünster (RM) and Gießen (GI). ~~Oxic incubations were conducted with two aggregate sizes (2-4 and 4-8mm) at 75% WFPS (GI) or 78% WFPS (RM).~~ Anoxic conditions were established after ~~7 days~~3 weeks of oxic incubation. Average (N_2O+N_2) fluxes from oxic and anoxic incubations served to calculate the anaerobic soil volume fraction ($ansvf_{cal}$). In comparison to the $ansvf_{cal}$, *ansvf* derived from X-Ray CT imaging $ansvf_{cal}$ result from the present study is also presented.

soil	WFPS	Aggregate size [mm]	$(N_2O+N_2)_{oxic}$ [µg N h^{-1} kg^{-1}] (parallel incubation)	$(N_2O+N_2)_{anoxic}$ [µg N h^{-1} kg^{-1}] (parallel incubation)	$ansvf_{cal}$	*ansvf* (present study)
RM	75-78	2-8	14±10	60±2	0.24±0.16	0.21
GI	75	2-8	61±97	136±18	0.45±0.71	0.13

Table with data for each replicate with average values of CO_2, N_2O and (N_2O+N_2) fluxes, O_2 saturation, total porosity, visible air content, connected air content (ε_{con}), anaerobic soil volume fraction (ansvf), diffusivity (D_{sim}) and product ratio (pr)

Table S4: Average values of CO_2, N_2O and (N_2O+N_2) fluxes, O_2 saturation, total porosity, visible air content (ε_{vis}), connected air content (ε_{con}), anaerobic soil volume fraction (*ansvf*), diffusivity (D_{sim}) and product ratio (*pr*, [$N_2O/(N_2O+N_2)$]) for the two soils (Gießen (GI) and Rotthalmünster (RM)), three water saturations and two aggregate sizes for three replicates. Standard error of the mean is shown in the brackets.

soil	WFPS[%]	Aggregate size [mm]	Replicate	CO_2-C [µg h^{-1} kg^{-1}] (n=28)	N_2O-N [µg h^{-1} kg^{-1}] (n=28)	(N_2O+N_2) [µg N h^{-1} kg^{-1}] (n=3)	O_2 [%air saturation] (n=7)	Total porosity [-]	ε_{vis} [-]	ε_{con} [-]	*ansvf* [-]	D_{sim} [m^2 s^{-2}]	*pr* (n= 1-3)
GI	63	2-4	a	406.30 (3.24)	0.22 (<0.01)	NA	47.19 (12.13)	0.20	0.20	0.19	0.003	$1.10\ 10^{-06}$	n.d.
GI	63	4-8	a	387.38 (2.83)	0.52 (0.07)	2.36 (NA)	53.79 (13.07)	0.19	0.19	0.19	0.004	$1.05\ 10^{-06}$	0.22 (n.d)
GI	75	2-4	a	528.74 (3.73)	21.28 (0.84)	31.45 (7.65)	46.27 (11.64)	0.18	0.13	0.12	0.037	$2.89\ 10^{-08}$	0.68 (0.14)
GI	75	4-8	a	463.32 (3.42)	20.14 (0.60)	30.21 (5.65)	59.24 (11.59)	0.19	0.14	0.10	0.246	$7.50\ 10^{-10}$	0.67 (0.12)
GI	85	2-4	a	317.57 (2.55)	33.68 (0.76)	39.78(3.94)	39.43 (9.42)	0.17	0.11	0.07	0.513	$1.54\ 10^{-10}$	0.85 (0.06)
GI	85	4-8	a	168.18 (2.30)	22.11 (0.59)	25.03 (2.79)	39.66 (12.20)	0.18	0.08	0.02	0.824	$1.40\ 10^{-10}$	0.88 (0.07)
GI	63	2-4	b	542.08 (8.62)	0.15 (<0.01)	5.09 (NA)	45.32 (10.48)	0.22	0.22	0.21	0.001	$1.11\ 10^{-06}$	0.03 (n.d.)
GI	63	4-8	b	506.33 (7.33)	0.71 (0.01)	2.62 (0.33)	57.38 (11.56)	0.21	0.21	0.21	0.001	$1.11\ 10^{-06}$	0.27 (0.03)
GI	75	2-4	b	610.95 (4.95)	20.73 (0.98)	36.37 (10.48)	62.33 (6.19)	0.18	0.13	0.12	0.068	$1.49\ 10^{-08}$	0.57 (0.14)
GI	75	4-8	b	525.22 (4.49)	19.51 (0.83)	32.34 (7.77)	71.78 (7.66)	0.19	0.14	0.10	0.312	$1.52\ 10^{-10}$	0.60 (0.12)
GI	85	2-4	b	95.47 (3.03)	12.48 (0.46)	22.98 (7.01)	28.45 (10.02)	0.18	0.12	<0.01	0.935	$1.23\ 10^{-09}$	0.54 (0.15)
GI	85	4-8	b	97.08 (2.71)	9.99(0.72)	20.82 (9.16)	34.16 (9.45)	0.18	0.11	<0.01	0.938	$1.82\ 10^{-10}$	0.48 (0.18)
GI	63	2-4	c	658.77 (5.38)	0.40 (0.01)	0.80 (0.10)	51.43 (9.55)	0.21	0.21	0.20	<0.001	$1.05\ 10^{-06}$	0.50 (0.04)
GI	63	4-8	c	615.87 (4.61)	2.63 (0.22)	3.81 (1.00)	70.19 (6.95)	0.20	0.20	0.20	<0.001	$1.08\ 10^{-06}$	0.69 (0.02)
GI	75	2-4	c	712.21 (5.89)	12.02 (0.90)	38.77 (10.84)	60.83 (8.62)	0.19	0.13	0.13	0.018	$3.88\ 10^{-09}$	0.31 (0.05)
GI	75	4-8	c	657.43 (5.30)	14.03 (1.07)	18.15 (4.37)	54.30 (14.00)	0.19	0.14	0.13	0.063	$7.38\ 10^{-09}$	0.77 (0.05)
GI	85	2-4	c	112.95 (7.61)	10.04 (1.16)	18.83 (9.96)	23.67 (10.43)	0.18	0.12	<0.01	0.910	$2.98\ 10^{-10}$	0.53 (0.21)
GI	85	4-8	c	111.59 (6.66)	7.80 (1.10)	18.29 18.87)	45.84 (10.25)	0.23	0.12	0.02	0.629	$2.75\ 10^{-10}$	0.43 (0.18)
RM	65	2-4	a	137.89 (0.65)	0.01 (n.d.)	NA	68.61 (7.14)	0.15	0.15	0.14	0.004	$2.51\ 10^{-07}$	n.d.
RM	65	4-8	a	164.47 (0.90)	0.10 (<0.01)	NA	35.75 (12.64)	0.16	0.16	0.15	0.005	$2.47\ 10^{-07}$	n.d.
RM	78	2-4	a	180.88 (1.57)	0.22 (0.01)	0.31 (0.10)	63.18 (10.22)	0.14	0.11	0.10	0.004	$1.66\ 10^{-08}$	0.71 (0.16)
RM	78	4-8	a	71.12 (1.00)	3.65 (0.21)	6.11 (1.32)	43.27 (11.97)	0.14	0.08	0.03	0.775	$2.34\ 10^{-11}$	0.60 (0.06)
RM	88	2-4	a	43.12 (0.19)	3.27 (0.11)	4.21 (0.73)	12.13 (8.11)	0.10	0.07	0.05	0.502	$7.31\ 10^{-11}$	0.78 (0.11)
RM	88	4-8	a	26.20 (0.12)	3.36 (0.08)	4.83 (0.48)	38.36 (11.27)	0.10	0.05	0.02	0.753	$5.53\ 10^{-09}$	0.70 (0.04)
RM	65	2-4	b	113.43 (0.75)	0.04 (<0.01)	NA	48.38 (11.00)	0.17	0.17	0.16	0.003	$2.10\ 10^{-07}$	n.d.
RM	65	4-8	b	118.83 (0.85)	0.05 (<0.01)	1.31 (NA)	42.40 (11.85)	0.15	0.15	0.14	0.005	$1.57\ 10^{-07}$	0.04 (n.d.)
RM	78	2-4	b	166.66 (1.95)	6.12 (0.30)	10.14 (3.34)	56.52 (8.62)	0.13	0.10	0.08	0.042	$1.02\ 10^{-08}$	0.60 (0.17)
RM	78	4-8	b	163.13 (0.92)	7.31 (0.19)	11.25 (1.98)	69.43 (9.15)	0.14	0.11	0.09	0.193	$2.13\ 10^{-08}$	0.65 (0.10)
RM	88	2-4	b	43.09 (0.20)	5.43 (0.09)	8.39 (1.01)	28.13 (9.56)	0.09	0.07	0.01	0.856	$1.04\ 10^{-11}$	0.64 (0.07)
RM	88	4-8	b	55.12 (0.70)	7.16 (0.16)	11.30 (1.74)	46.26 (9.60)	0.14	0.07	0.01	0.860	$3.65\ 10^{-11}$	0.63 (0.09)

RM	65	2-4	c	183.25 (0.70)	n.d.	NA	53.25 (14.68)	0.17	0.17	0.16	0.003	$2.10\ 10^{-07}$	n.d.
RM	65	4-8	c	190.89 (0.82)	n.d.	NA	68.71 (15.40)	0.16	0.16	0.15	0.003	$2.19\ 10^{-07}$	0.11 (n.d.)
RM	78	2-4	c	175.34 (0.30)	6.51 (0.18)	10.12 (2.29)	57.79 (6.92)	0.14	0.11	0.08	0.203	$4.00\ 10^{-09}$	0.64 (0.13)
RM	78	4-8	c	193.83 (1.27)	7.04 (0.46)	12.29 (3.66)	58.57 (12.57)	0.14	0.11	0.10	0.062	$2.28\ 10^{-08}$	0.57 (0.12)
RM	88	2-4	c	65.58 (0.40)	6.53 (0.07)	12.80 (2.94)	27.69 (8.80)	0.11	0.05	0.02	0.720	$1.45\ 10^{-11}$	0.51 (0.12)
RM	88	4-8	c	549.33 (0.22)	6.27 (0.12)	9.36 (1.24)	41.41 (9.23)	0.16	0.08	0.03	0.613	$5.19\ 10^{-10}$	0.67 (0.08)

242 n.d.: not detectable; NO and N_2 concentration was below detection limit for IRMS analysis, thus calculation of *pr* was impossible. NA: not applicable

References

Benjamini, Y., and Hochberg, Y.: Controlling the False Discovery Rate: A Practical and Powerful Approach to Multiple Testing, Journal of the Royal Statistical Society. Series B (Methodological), 57, 289-300, 1995.

Deepagoda, T., Moldrup, P., Schjonning, P., de Jonge, L. W., Kawamoto, K., and Komatsu, T.: Density-Corrected Models for Gas Diffusivity and Air Permeability in Unsaturated Soil, Vadose Zone J., 10, 226-238,

Lewicka-Szczebak, D., Well, R., Giesemann, A., Rohe, L., and Wolf, U.: An enhanced technique for automated determination of ^{15}N signatures of N_2, (N_2+N_2O) and N_2O in gas samples, Rapid Commun. Mass Spec., 27, 1548-1558, https://doi.org/10.1002/rcm.6605, 2013.

Millington, R., and Quirk, J. P.: Permeability of porous solids, Transactions of the Faraday Society, 57, 1200-&, https://doi.org/10.1039/tf9615701200, 1961.

Millington, R. J., and Quirk, J. M.: Transport in porous media, in: F.A. Van Beren et. al (ed.), Trans. Int. Congr. Soil Sci., 7th, Madison, WI. 14–21 Aug, Elsevier, Amsterdam, 97–106, 1960.

Moldrup, P., Olesen, T., Gamst, J., Schjonning, P., Yamaguchi, T., and Rolston, D. E.: Predicting the gas diffusion coefficient in repacked soil: Water-induced linear reduction model, Soil Sc. Soc. Am. J., 64, 1588-1594, https://doi.org/10.2136/sssaj2000.6451588x, 2000.

Spott, O., Russow, R., Apelt, B., and Stange, C. F.: A ^{15}N-aided artificial atmosphere gas flow technique for online determination of soil N_2 release using the zeolite Köstrolith SX6®, Rapid Commun. Mass Spec., 20, 3267-3274, https://doi.org/10.1002/rcm.2722, 2006.

Well, R., Burkart, S., Giesemann, A., Grosz, B., Köster, J. R., and Lewicka-Szczebak, D.: Improvement of the ^{15}N gas flux method for in situ measurement of soil denitrification and its product stoichiometry, Rapid Commun. Mass Spec., 33, 437-448, https://doi.org/10.1002/rcm.8363, 2019.

Wiegmann, A., and Bube, K. P.: The explicit-jump immersed interface method: Finite difference methods for PDEs with piecewise smooth solutions, SIAM J. Numer. Anal., 37, 827-862, https://doi.org/10.1137/S0036142997328664, 2000.

Wiegmann, A., and Zemitis, A.: EJ-HEAT: A fast explicit jump harmonic averaging solver for the effective heat conductivity of composite materials, Berichte des Fraunhofer ITWM, 94, 2006.

Formatiert: Abstand Nach: 4 Pt.